1074

NATIONAL ADVISORY COMMITTEE FOR AERONAUTICS

TECHNICAL NOTE

No. 1074

TESTS OF A FULL-SCALE HORIZONTAL TAIL SURFACE

IN THE LANGLEY 16-FOOT HIGH-SPEED TUNNEL

By Carl F. Schueller, Peter F. Korycinski
and H. Kurt Strass

Langley Memorial Aeronautical Laboratory
Langley Field, Va.

NACA

Washington
May 1946

NATIONAL ADVISORY COMMITTEE FOR AERONAUTICS

———

TECHNICAL NOTE No. 1074

———

TESTS OF A FULL-SCALE HORIZONTAL TAIL SURFACE

IN THE LANGLEY 16-FOOT HIGH-SPEED TUNNEL

By Carl F. Schueller, Peter F. Korycinski
and H. Kurt Strass

SUMMARY

        Tests to determine the aerodynamic characteristics
of a full-scale semispan horizontal tail surface of a
fighter-type airplane have been conducted in the Langley
16-foot high-speed tunnel. The tests were carried to a
maximum Mach number of 0.7 except for model configura-
tions for which the maximum allowable loads were reached
at lower speeds. The results presented show the effects
of elevator nose shape, elevator trailing-edge angle,
and trailing-edge strips on the aerodynamic character-
istics of the model. Results are also given for a few
measurements of the external and internal elevator pres-
sures and the extent of laminar flow on the stabilizer.

        Increasing the Mach number from 0.2 to 0.7 resulted
in a marked increase (-0.0015 to -0.0032) in the rate of
change of hinge-moment coefficient with elevator deflec-
tion, a small increase (0.0025 to 0.0027) in the rate of
change of hinge-moment coefficient with angle of attack
and an appreciable loss (0.51 to 0.34) in elevator
effectiveness.

        The incremental changes in elevator hinge-moment
characteristics due to modifying the elevator nose con-
tour were of about the same magnitude as would be pre-
dicted by the use of recently published methods.

INTRODUCTION

Past experience has shown that surface irregularities and deflections have detrimental effects on the aerodynamic characteristics of horizontal tail surfaces, particularly at high speeds. Accurate estimates of the characteristics of tail surfaces for high-speed airplanes therefore require tests of full-scale models which are reproductions of the tail surface to be used on the airplanes. The model used in these tests was built by conventional manufacturing methods and was for use on an experimental airplane after completion of the wind-tunnel investigation.

The original metal-covered elevator was tested through a range of Mach numbers of 0.2 to 0.7 to determine the aerodynamic characteristics. A few tests were also made to determine the extent of laminar flow, the external and internal elevator pressures, and the effect on the aerodynamic characteristics of trailing-edge strips and of lowering the elevator with respect to the stabilizer.

Several profile modifications of a full-scale wooden elevator were tested at low speed to obtain the effect of nose shape and trailing-edge angle modifications on the elevator characteristics.

COEFFICIENTS AND SYMBOLS

C_D drag coefficient (D/qS)

C_h hinge-moment coefficient $\left(H/q\bar{c}_e^2 b_e\right)$

C_L lift coefficient (L/qS)

C_m pitching-moment coefficient $\left(\dfrac{M_{c/4}}{qS}\right)$

where

D   drag of horizontal semispan tail surface

H   hinge moment of elevator

L   lift of horizontal semispan tail surface

$M_{c/4}$ pitching moment about quarter-chord point of mean
         aerodynamic chord

b   span, inches

c   chord of horizontal tail, inches

$\overline{c}_e$ root-mean-square of elevator chord behind hinge
         line, inches

q   dynamic pressure $\left(\frac{1}{2}\rho V^2\right)$

ρ density, slugs per cubic foot

V   velocity, feet per second

S   total area, square feet

and

P   pressure coefficient $\left(\dfrac{p - p_o}{q_o}\right)$

p   static pressure at any point

R   Reynolds number

M   Mach number

α angle of attack of stabilizer

δ angle of elevator chord with respect to stabilizer
         chord (trailing edge down is positive)

$\emptyset$ included angle at elevator trailing edge

and

$$\left(\frac{\partial \alpha}{\partial \delta}\right)_{C_L} = \frac{C_{L_\delta}}{C_{L_\alpha}}$$

$$C_{L_\alpha} = \left(\frac{\partial C_L}{\partial \alpha}\right)_\delta$$

$$C_{L_\delta} = \left(\frac{\partial C_L}{\partial \delta}\right)_\alpha$$

$$C_{h_\alpha} = \left(\frac{\partial C_h}{\partial \alpha}\right)_\delta$$

$$C_{h_\delta} = \left(\frac{\partial C_h}{\partial \delta}\right)_\alpha$$

$$C_{m_\alpha} = \left(\frac{\partial C_m}{\partial \alpha}\right)_\delta$$

$$C_{m_\delta} = \left(\frac{\partial C_m}{\partial \delta}\right)_\alpha$$

$$\left(\frac{\partial C_m}{\partial C_L}\right)_\alpha = \frac{C_{m_\alpha}}{C_{L_\alpha}}$$

$$\left(\frac{\partial C_m}{\partial C_L}\right)_\delta = \frac{C_{m_\delta}}{C_{L_\delta}}$$

The subscripts outside the parentheses represent the factors held constant in the determination of the parameters.

Subscripts:

e   elevator

i   internal

o   free stream

b   balance

DESCRIPTION OF MODEL

The model was a full-scale semispan horizontal tail surface of a fighter-type airplane. The airfoil was made according to the NACA 66-009 profile, modified to have a straight contour beyond the 72-percent-chord station. The physical characteristics of the model are given in table I and figure 1.

Stabilizer.- The stabilizer was of metal construction and metal covered. (See fig. 2.) All rivets were flush and the surface had been filled, rubbed with abrasive cloth, and waxed to increase the surface smoothness; however, considerable surface waviness existed. The gap between the elevator and stabilizer was approximately 1/4 inch and was constant for all elevator angles. In order to reduce undesirable air flow through the elevator hinge pockets, the model included cover plates, which were attached to the top and bottom of each stabilizer hinge bracket.

Elevators.- The chordwise and spanwise dimensions of all the elevators tested were equal. The hinge line was located at 72.0 percent of the chord of the horizontal tail and the overhang was 48 percent of the elevator chord $\left(\dfrac{c_b}{c_e} = 0.48\right)$. No trim tab is used on the elevator of this airplane because the angle of incidence of the stabilizer is adjustable in flight.

The metal elevator was of aluminum construction with no vent or drain holes. The nose shape was semi-elliptical, and the contour was a straight taper behind the hinge line, resulting in a trailing-edge angle of approximately 13°.

Elevators 1, 2, 3, and 4 were constructed of spruce and incorporated systematic modifications to the elevator profile (fig. 3). Elevator 1 had a blunt nose and straight taper behind the hinge line $(\emptyset = 13°)$. Elevator 2 had a blunt nose and a cusped contour behind the

hinge line (∅ = 7°). Elevator 3 had a modified blunt
nose and a cusped contour behind the hinge line (∅ = 7°).
Elevator 4 had a semielliptical nose, of the same con-
tour as the metal-covered elevator, and a cusped contour
behind the hinge line (∅ = 7°). The coordinates of
these elevators are given in table II.

Examination of the stabilizer and metal elevator
showed that the center line of hinge-bearing in the sta-
bilizer brackets was approximately three thirty-seconds
of an inch above the chord line. On the other hand the
hinge pins for the metal elevator were found to be slightly
above the chord line. As a result of these structural
irregularities, the upper surface of the elevator pro-
jected approximately one-sixteenth of an inch above the
contour of the stabilizer for neutral elevator. The
effect of these structural irregularities and the modi-
fications made to compensate for them will be discussed
later.

APPARATUS AND METHODS

Model installation.- Inasmuch as a semispan model
was used, it was necessary to locate the center line of
the horizontal tail surface in the plane of the tunnel-
wall flat to produce air-flow conditions more closely
simulating those of flight. (See figs. 1 and 2.)
Labyrinth-type seals were used where the model support
went through the tunnel-wall flat to reduce to a minimum
the leakage of air from the test chamber to the tunnel.

Hinge-moment measurement.- The elevator control
tube was extended so that it passed through the tunnel
flat and two self-alining bearings mounted on the tunnel
balance frame. The elevator hinge moment was transferred
through the elevator torque tube to a 6-inch crank and
then through a jackscrew to the platform of a scale. The
jackscrew was also used to vary the elevator angle. The
platform scale was attached rigidly to the tunnel balance
frame and, since all other related parts were also
attached to the tunnel balance frame, there was no possi-
bility of the hinge-moment measurements interfering with
the measurements of lift, drag, and pitching moment.
All force and moment data were recorded simultaneously.

Elevator angle measurement.- An autosyn was used to
measure the elevator angle. The transmitter was attached
rigidly to the stabilizer at the inboard hinge cut-out.
A small pinion gear on the transmitter shaft was driven
by a large gear sector, which was rigidly attached to the
root of the elevator. Thus, any elevator deflection was
multiplied by the gear ratio (approximately 12:1) and
transmitted electrically to the receiver. A calibrated
dial attached to the receiver provided a continuous
visual indication of the elevator angle. A templet was
used to check the zero reading of the autosyn indicator.
This system measured the elevator root angle within ±0.1°.

Angle-of-attack measurement.- An inclinometer
located on a reference surface of the model support
system was used to measure the angle of attack of the
stabilizer. The measurement of the root angle of the
stabilizer is believed to be accurate within ±0.05°.

Pressure measurements.- Pressure measurements over
the nose and top surface of the metal-covered elevator
were made by the use of a pressure belt (0.090-inch-
diameter tubes) located approximately 47 inches from the
center line of the airplane (station 47). External pres-
sures were also measured behind the middle hinge pocket
on the top surface of the elevator by means of a small
pressure belt. These pressure belts are believed to
have no important effect on the pressure distributions.

The internal pressure of the elevator was measured
by open-end tubes located in two elevator panels. One
tube was located near the inboard end of the elevator
(station 30) and the other in the panel adjacent to and
on the inboard side of the middle hinge pocket (station 47).

Trailing-edge strips.- Strips of $\frac{1}{8}$-inch- or $\frac{1}{16}$-inch-
diameter tubing were attached to both surfaces of the
metal elevator at the trailing edge. The method of
attaching the tubing to the elevator is shown in fig-
ure 4. Strips that were full span, half span, and
quarter span in length were tested. The length of the
trailing-edge strips was varied by cutting equal lengths
from the root and tip ends of the strips. (See fig. 4.)

Transition strips.- The extent of laminar flow over
the stabilizer, with metal elevator, was determined by

fixing the transition with $\frac{1}{2}$-inch-wide strips of carbo-
rundum on the top surface of the stabilizer at constant
percentage of chord stations. Shellac was first applied
to the surface as a spanwise strip on which No. 60
powdered carborundum was evenly distributed. Upon com-
pletion of the tests with this transition strip, it was
removed and the process was repeated at a more forward
station. At the 5-percent-chord station tests were made
with the strip on the top surface and also with strips
on both the top and bottom surfaces.

TESTS

    Test data for the metal elevator were generally
obtained for angles of attack of -3°, 0°, 3°, 6°, and 9°;
elevator deflections of -13°, -8°, -4°, -1°, 0°, 2°, 5°,
9°, and 14°; and M = 0.20, 0.35, 0.45, 0.50, 0.55, 0.60,
0.65, and 0.70 with the original hinge position. The
possible combinations of these variables were limited
by the maximum allowable load on the model. A few tests
also were made with the stabilizer hinge brackets lowered
3/32 inch.

    The wooden elevators were tested only at moderate
speeds and a small range of angle of attack and elevator
angles. Tests to determine the effect of trailing-edge
angle (elevators 1 and 2) were made with the original
hinge location. Tests to determine the effects of nose
shape (elevators 2, 3, and 4) were made with the sta-
bilizer hinge bracket lowered 3/32 inch. Tests of ele-
vator profile modifications, trailing-edge strips, and
transition strips included only limited combinations of
angle of attack, elevator angle, and speed, usually
α = -3° to 3°, δ = -8° to 9°, and M = 0.35.

REDUCTION OF DATA

    The data presented in this report have been corrected
for tunnel-wall effects by the use of the reflection-
plane theory given in reference 1. The projected frontal
area of the model was such a small part of the tunnel
area that tunnel-constriction corrections were negligible.
Also, corrections to pitching moment due to model deflec-
tion and balance-frame deflection were found to be

negligible. The corrected data were cross-plotted and the values at selected angles of attack and elevator angles were then plotted against Mach number. The average dynamic pressures and average Reynolds numbers corresponding to the test Mach numbers are shown in figure 5. The Reynolds number is based on the calculated mean aerodynamic chord of 4.27 feet. The results herein are generally plotted against Mach number rather than velocity or dynamic pressure because Mach number is considered to be the dominating variable. The effects shown in these plots, however, include effects due to distortion of the model under load and are not entirely compressibility effects.

Tests were made with approximately a $\frac{1}{4}$-inch gap around the model support at the tunnel flat, with this gap reduced to a minimum by the use of a labyrinth seal, and with the gap completely sealed with flexible tape. These tests indicated that corrections to the aerodynamic coefficients due to air leakage from the test chamber to the tunnel for the various leak conditions tested were negligible for this setup. All tests were made with the labyrinth-type seal around the model end gap.

RESULTS AND DISCUSSION

Basic Data with Metal Elevator

Effect of angle of attack.- The variation of the aerodynamic coefficients C_L, C_D, and C_m over a wide range of angle of attack at low speed with the metal elevator is shown in figure 6 for $\delta = -0.5°$ and $10.6°$. The low value of maximum C_L obtained prompted a tuft study to determine the origin and progress of the stall. At an angle of attack of $11°$ a local area of separated flow appeared near the leading edge, centered about 1 foot in from the stabilizer tip and extending over about 1 foot of the span. As the angle of attack was increased, the separation spread backward along the chord and inboard toward the stabilizer root.

Effect of Mach number.- The variation of the aerodynamic characteristics of the metal elevator with Mach

number is shown in figure 7 for $\alpha = -3°$, $0°$, $3°$, $6°$, and $9°$ and a maximum test range of $\delta = 14°$ to $-13°$. The increase in C_D with Mach number shown in this figure does not indicate that the critical speed of the tail surface was attained in these tests. The pitching-moment and lift coefficients would be expected, from Glauert's theory, to increase approximately according to the factor $\left(1 - M^2\right)^{-1/2}$; however, figure 7 does not show an increase of this order of magnitude. In fact, for some model configurations at small values of α and large values of δ, the lift coefficients decrease with increasing Mach number, and this decrease is believed to result from twist of the stabilizer when the lift was obtained by deflecting the elevator. The elevator hinge-moment coefficient generally increased with increasing Mach number for $\delta = 9°$ to $-8°$. This increase was much more rapid than the increase obtained by the use of Glauert's factor $\left(1 - M^2\right)^{-1/2}$. The failure of the test data to increase according to Glauert's factor is not unexpected since this theory does not take into account the effects of boundary layer and structural deformations. At Mach numbers beyond the test range some changes in all coefficients are likely to occur.

Aerodynamic Parameters of Metal Elevator

Lift.- The variation of the lift parameters C_{L_α} and C_{L_δ} of the metal elevator with Mach number is shown in figure 8. The increase of the parameter C_{L_α} with Mach number is less than would be predicted by the use of Glauert's factor and no critical condition is apparent up to a Mach number of 0.70. The gradual decrease of C_{L_δ} with Mach number is an undesirable characteristic and is believed to be due to the gap (0.005c) between the stabilizer and elevator leading edge and partly to the elevator twist. Should the value of C_{L_δ} be used as an indication of elevator effectiveness, figure 8(a) would indicate that the loss in elevator effectiveness is small as the airspeed is increased; however, the ratio $\dfrac{C_{L_\delta}}{C_{L_\alpha}} = \dfrac{\partial \alpha}{\partial \delta}$ is usually used as a criterion of elevator effectiveness. The variation of $\partial \alpha / \partial \delta$ with Mach number as shown in figure 8(b) indicates

that the elevator effectiveness decreased from 0.51 at
M = 0.20 to 0.34 at M = 0.70. Since C_{L_α} and C_{L_δ}
would be expected to increase with speed and C_{L_δ}
actually decreases with speed, the loss of elevator effec-
tiveness with increasing speed is ascribed to the decrease
in C_{L_δ}. As mentioned previously, the decrease in C_{L_δ}
with increasing speed is believed to result primarily
from the gap between the rear part of the stabilizer and
the elevator leading edge. This impression is further
substantiated by a comparison of the results of tests of
another full-scale tail surface at high speeds (refer-
ence 2) with the present model. The only important
difference between the two horizontal tail surfaces as
regards the change in C_{L_δ} with speed is the use of an
elevator seal on the model of reference 2. Any differences
in the variation of C_{L_δ} with speed for the two models
must therefore be an effect of the elevator-gap con-
figuration. In figure 24(a) of reference 2, the value
of C_{L_δ} is shown to increase with increasing speed up
to the maximum test speed M = 0.68 when the elevator
gap was sealed and the elevator with no appreciable
fabric distortion (elevator 1) was tested.

The theoretical elevator effectiveness has been
calculated according to the theory of reference 3 and is
20 percent higher than the experimental value obtained
at M = 0.20. Since the thin-airfoil theory applies to
flaps hinged at the leading edge and no correction is
made for the increase in lift due to the balance area,
the elevator with the balance area would be expected to
have a higher effectiveness. Reasonable agreement is
obtained, however, between the low-speed value of $\partial\alpha/\partial\delta$
of 0.51 for these tests and the experimental value of
0.55 of reference 4.

Pitching moment.- The variation of pitching-moment
parameters with Mach number is shown in figure 9. The
parameters C_{m_α} and C_{m_δ} (fig. 9) increase in absolute
value with increasing Mach number. The parameter
$\left(\partial C_m/\partial C_L\right)_\alpha$ gives the position of the aerodynamic center
with respect to the quarter-chord point of the calculated
mean aerodynamic chord. The variation of the parameter
$\left(\partial C_m/\partial C_L\right)_\alpha$ with Mach number is presented in figure 9.
When the lift is obtained by changing the angle of

attack, $\left(\partial C_m / \partial C_L\right)_\delta$ at $\delta = 0°$,   the aerodynamic center
of the airfoil shifts forward from 0.227c at $M = 0.20$
to 0.160c at $M = 0.70$. When the lift is obtained by
changing the elevator angle at $\alpha = 0°$,   the aerodynamic
center of the airfoil shifts rearward from 0.520c at
$M = 0.20$ to 0.670c at $M = 0.70$. However, these changes
in the location of the aerodynamic center will have neg-
ligible effect on the stability and control of the airplane.

Hinge moment.- The effect of increasing Mach number
on the elevator hinge-moment parameters is shown in fig-
ure 10. In general, the overbalance of C_{h_α} and the
underbalance of C_{h_δ} increased with increasing Mach
number. In the absence of boundary-layer changes, the
elevator hinge-moment coefficient might logically be
assumed to increase in absolute value with speed according
to Glauert's factor $\left(1 - M^2\right)^{-1/2}$. However, the increase
in C_{h_δ} with Mach number is approximately three times
this factor at $M = 0.70$. Furthermore, the increase
in C_{h_δ} represents an increase of approximately 100 per-
cent in the hinge-moment coefficient. (See reference 2.)
Also shown in figure 10 are the values for zero and
100 percent aerodynamic balance and balance effective-
ness. The values for zero aerodynamic balance have been
calculated according to the theory presented in refer-
ences 5 and 6 and, as such, do not include compressibility
effects. However, the low-speed values have been extended
through the speed range tested to provide an approximate
criterion for judging the experimental values.

Effect of Trailing-Edge Angle

The low-speed values of C_{h_α} and C_{h_δ} obtained
with the metal elevator (trailing-edge angle 13°) were
0.0020 and -0.0015, respectively. The results of tests
made at the Langley Laboratory of a scale model of the
complete airplane and experience with flight investiga-
tions on other airplanes have shown that the value of
C_{h_α} should be approximately zero in order to avoid adverse
effects on the stability and control characteristics,
particularly in gusty air. Preliminary calculations
based on unpublished data indicated that zero C_{h_α} could
be obtained by decreasing the trailing-edge angle from
approximately 13° to 7°. This change in elevator shape
was obtained by the use of solid wood elevators and is
illustrated in figure 3.

    <u>Hinge moment</u>.- The effect of trailing-edge angle
on the elevator hinge-moment coefficient is shown in
figure 11 for three angles of attack and $M = 0.35$. The
nonlinearity of these curves prevents the exact use of
the usual parameters, but the 6° change in elevator
trailing-edge angle resulted in changes in the parameters
of approximately $\Delta C_{h_\delta} = -0.0013$ and $\Delta C_{h_\alpha} = -0.0026$.
The change in C_{h_α} due to reducing the trailing-edge
angle was of the desired magnitude, but the accompanying
increase in C_{h_δ} was undesirable. The undesirable
increase in C_{h_δ} due to reducing the trailing-edge angle
may be nullified with no appreciable change in C_{h_α} by
changing the elevator nose shape. (See section entitled
"Effect of Nose Shape.")

    <u>Effect on drag</u>.- The variation of the drag coeffi-
cient for elevators 1 and 2 ($\emptyset = 13°$ and $7°$, respec-
tively) with elevator angle is presented in figure 12
for three angles of attack and $M = 0.35$. The increase
in drag for a given increment of elevator deflection is
slightly more for elevator 2 ($\emptyset = 7°$) than for elevator 1
($\emptyset = 13°$).

    <u>Effect on lift</u>.- In general, a decrease in elevator
trailing-edge angle was accompanied by a slight increase
in lift. Reducing the trailing-edge angle from 13° to 7°
increased C_{L_α} from 0.061 to 0.064 and C_{L_δ} from 0.031
to 0.032.

    <u>Effect on pitching moment</u>.- Reducing the trailing-
edge angle from 13° to 7° caused the center of lift to
be shifted rearward. The center of lift shifted from
22.6 to 24.2 percent of the mean aerodynamic chord for
$\delta = 0°$ when the lift was varied by changing the angle
of attack. The center of lift was shifted from 56 to
57.7 percent of the mean aerodynamic chord for $\alpha = 0°$
when the lift was varied by changing the elevator angle.
These changes agree qualitatively with other investi-
gations (reference 7).

<center>Effect of Nose Shape</center>

    The results of these tests for trailing-edge con-
figurations showed that the desired value of C_{h_α} could

be obtained with a trailing-edge angle of approximately
7°. The reduction in trailing-edge angle, however,
caused an appreciable increase (-0.0013) in the value of
C_{h_δ}. Since the original value of C_{h_δ} obtained for the
metal elevator (-0.0015) was considered satisfactory by
the manufacturer, it was desirable to reduce the new value
of C_{h_δ}. Reference 8 shows that the value of C_{h_δ} can
be changed, without appreciably affecting the value of
C_{h_α}, by altering the elevator nose shape. Accordingly,
systematic alterations were made to the nose profile
until a satisfactory value of C_{h_δ} was obtained. (See
fig. 3.)

Hinge moment.- The effect of the nose modifications
on the hinge-moment coefficient at a Mach number of 0.35
is shown in figures 13 and 14. The nonlinearity of the
variation of the hinge-moment coefficient with elevator
angle prevents an exact measure of the parameter C_{h_δ}.
Also, the difference in structural stiffness between the
wooden and metal elevators and the asymmetry of the metal
elevator prevents a direct comparison of the hinge-moment
parameters of the two elevators. Therefore, elevator 4,
which had a semielliptical nose profile like the metal
elevator, is used as a reference and only the incremental
changes in C_{h_δ} and C_{h_α} due to nose modifications are
presented. Figures 13 and 14 indicate that modifying
the elevator nose profile to modified blunt shape (ele-
vator 3) results in $\Delta C_{h_\delta} = 0.0010$ and $\Delta C_{h_\alpha} = 0.0002$,
approximately, and modifying the elevator nose to the
blunt shape (elevator 2) results in $\Delta C_{h_\delta} = 0.0020$ and
$\Delta C_{h_\alpha} = 0.0004$; consequently, an elevator that has a
slightly greater balance-moment area than elevator 3 will
provide the desired decrease in C_{h_δ} of 0.0013 and so
nullify the adverse effect of reducing the trailing-edge
angle to 7°. The tests of the wooden elevator therefore
indicate that the desired values of $C_{h_\alpha} \approx 0$ and
$C_{h_\delta} = -0.0015$ at $M = 0.35$ may be obtained if the original
metal elevator profile is modified so that it has a modi-
fied blunt nose shape (elevator 3) and a cusped contour
behind the hinge line (elevator 2).

The incremental changes in C_{h_δ} due to the elevator
nose-contour modifications are of the same order of
magnitude as would be calculated by the method of

reference 8.   As might be expected, very poor agreement
is obtained when the value of C_{h_δ} for any one elevator

is calculated from the unbalanced section flap data and
corrected for balance effects by this method.   More
precise methods for correcting section hinge-moment data
to finite aspect ratio are being developed at the present
time.

Lift.- The effect of elevator nose contour on C_{L_δ}
is shown in figure 15 at $\delta = 0°$, $M = 0.35$,   and $\alpha = -3°$
to $3°$.   Figure 15 shows that the lift increases slightly
as the surface discontinuity between the rear portion of
the stabilizer and the elevator nose is reduced because,
as the contour of the tail surface approaches that of
the true airfoil, optimum pressure distribution and lift
are obtained.

Drag.- The effect of elevator nose contour on drag
is also shown in figure 15.   The drag increases slightly
as the surface discontinuity between the rear portion of
the stabilizer and the elevator nose is increased.

Pitching moment.- The effect of elevator nose con-
tour on the pitching moment was not appreciable and no
data are presented.

Effect of Trailing-Edge Strips

Temporary changes in elevator characteristics are
often made by the use of trailing-edge strips.   An inves-
tigation was therefore undertaken to determine, for this
full-scale tail surface, the combinations of length and
diameter of trailing-edge strips that could be used on
the original elevator as a temporary expedient to obtain
$C_{h_\alpha} = 0$.   Various lengths of $\frac{1}{8}$-inch- and $\frac{1}{16}$-inch-diameter
strips were tested at $M = 0.35$ and $\alpha = -3°$, $0°$, and $3°$.

Hinge moment.- Figures 16 and 17 show the variation
of hinge-moment coefficient with elevator angle for
various lengths of $\frac{1}{8}$-inch- and $\frac{1}{16}$-inch-diameter trailing-
edge strips, respectively, at $\alpha = -3°$, $0°$, $3°$, and
$M = 0.35$. Decreasing the length of the strip decreases
the slope of the hinge-moment curves, and no abrupt
changes in the trend of the curves occur.   The data

presented in these figures have been used to obtain the hinge-moment parameters C_{h_α} and C_{h_δ} shown in figure 18. The desired value of $C_{h_\alpha} = 0$ can be obtained by use of a $\frac{1}{8}$-inch-diameter trailing-edge strip extending across 24 percent of the span or a $\frac{1}{16}$-inch-diameter strip extending across 38 percent of the span and centrally located on the elevator, at the expense, however, of an undesirable increase in C_{h_δ}. The effect of speed on the effectiveness of the trailing-edge strips is shown in figure 19. No serious change of hinge-moment coefficient or C_{h_α} occurs up to $M = 0.65$ with the full-span $\frac{1}{8}$-inch-diameter strips on the elevator trailing edge.

Of interest is the fact that the effects of the trailing-edge strips on the hinge-moment-coefficient parameters, C_{h_α} and C_{h_δ}, and the lift parameter C_{L_δ} are directly opposite to the effects due to beveling the trailing edge; that is, the use of trailing-edge strips results in increases in the values of C_{h_α}, C_{h_δ}, and C_{L_δ}, whereas beveling a trailing edge causes decreases in the values of these parameters.

Lift.- The effect of varying the length of the trailing-edge strips on lift coefficient is shown in figure 20 for the $\frac{1}{8}$-inch-diameter strip and in figure 21 for the $\frac{1}{16}$-inch-diameter strip. The use of full-span strips of either diameter results in an appreciable increase in lift at the high elevator angles. This increase in lift, however, affects only the value of C_{L_δ}, the value of C_{L_α} remaining practically constant. The value of C_{L_δ} increases linearly with strip length; the increase for the $\frac{1}{8}$-inch- and $\frac{1}{16}$-inch-diameter strips is 17 and 15 percent, respectively, when the strip length is increased from zero-span length to full-span length.

Drag.- The effect of the length of the trailing-edge strips on drag coefficient for $\frac{1}{8}$-inch- and $\frac{1}{16}$-inch-diameter strips is shown in figures 22 and 23, respectively. In general, the increase in drag due to

lengthening the strips for the $\frac{1}{8}$-inch-diameter strips is double the increase which occurred with the $\frac{1}{16}$-inch-diameter strips. The maximum increase in drag coefficient measured with $\frac{1}{8}$-inch-diameter, full-span strips was 13 percent.

Pitching moment.- The center of lift was shifted from 23 percent to 25 percent of the mean aerodynamic chord for $\delta = 0^\circ$ when the lift was increased by changing the angle of attack. The maximum shift in the aerodynamic center was from 52 percent to 58 percent of the mean aerodynamic chord for $\alpha = 0^\circ$ when the lift was increased by changing the elevator angle.

Effect of Lowering the Elevator with

Respect to the Stabilizer

The data presented in the section entitled "Basic Data with Metal Elevator" indicated that the metal elevator trimmed at approximately -5° for $\alpha = 0^\circ$, which is believed to be a result of an error in the hinge location (see "Description of Model") and possibly some asymmetry in the elevator contour. A limited number of tests were therefore made with the metal elevator lowered to be more nearly alined with the stabilizer in order to determine the effect of this change.

Hinge moment.- The effect of lowering the hinge line on the elevator hinge moment is shown in figure 24 for three angles of attack and $M = 0.35$. The new hinge position results principally in a shift of the hinge-moment-coefficient curves for a limited range of elevator angles. The elevator trim angle at $\alpha = 0^\circ$ is changed from -5° to -1°.

Effect on lift, drag, and pitching moment.- No data are presented to show the effect of lowering the hinge line on C_L, C_D, and C_m because the effect was negligible.

Transition Strips

An investigation to determine the extent of laminar flow on the stabilizer was undertaken. Carborundum strips which are described in detail under "Methods and Apparatus" were used to fix the transition location.

Effect on drag.- Fixing the transition ahead of its normal location should result in an appreciable increase in drag. No pronounced increase in drag occurred as the transition strip was moved forward on the upper surface (fig. 25) to the 0.05c location, and it is therefore concluded that only a limited region of laminar flow existed, possibly 0.10c. The lack of laminar flow cannot be attributed to tunnel air-stream turbulence, since the turbulence factor for this tunnel is of the same order of magnitude as the factor for the low-turbulence tunnel, and extensive laminar flow is usually obtained on smooth models. Surface irregularities near the stabilizer nose, particularly a spanwise joint at 0.10c, are probably responsible for fixing the transition location. Figure 26 shows the effect on drag of locating the transition strips on the upper and lower surface of the stabilizer at 5 percent chord at $\delta = 0°$ for $M = 0.20, 0.45,$ and 0.60. The increment of drag caused by the transition strips remains almost constant for $\alpha = -3°$ to $3°$ and $M = 0.20$ to 0.60 and essentially equal to the increase shown in figure 25.

Effect on elevator hinge moment.- The effect on elevator hinge moment of moving the transition strip forward is shown in figure 25 for $\delta = 0°$ and $4°$, $\alpha = 0°$, and $M = 0.45$. The hinge moment decreases slightly as the transition strip is moved forward. This effect is believed to be due to thickening of the boundary layer.

Effect on lift and pitching moment.- The effect of the transition-strip location on C_L and C_m was not appreciable for any of the conditions tested.

Aerodynamic Hysteresis

Attempts to check some of the hinge-moment data revealed apparent discrepancies, the magnitude of which appreciably exceeded the accuracy of the measurements. An investigation to determine the source of these discrepancies revealed that, for a given model configuration,

two values of hinge moment could be obtained, depending on the direction from which the desired elevator angle was approached.

Effect on hinge moment.- Figure 27 shows the aerodynamic hysteresis effect for elevator 1. In general, the hysteresis was present for about $15°$ of the elevator travel. The maximum deviation due to hysteresis is approximately $2°$ of elevator angle. The hysteresis effect shown in figure 27 is representative of all of the elevators tested which had a straight contour behind the hinge line. Cusping the elevator contour behind the hinge line and so reducing the trailing-edge angle to $7°$ resulted in the virtual disappearance of the aerodynamic hysteresis. Also the hysteresis disappeared for all practical purposes at Mach numbers greater than about 0.65. The aerodynamic hysteresis is probably related to local boundary-layer separation on the rear part of the elevator. It is an obviously undesirable phenomenon, which would possibly necessitate continuous small adjustments of the airplane trimming mechanism in flight.

Effect on lift, drag, and pitching moment.- Inasmuch as the hysteresis was related to the elevator contour behind the hinge line, only a fraction of the total area was affected. As would be expected, the effect on lift, drag, and pitching moment was found to be negligible and no data are presented.

Elevator Pressure

The metal skin on both the upper and lower surfaces of the elevator at station 50 (fig. 28) bulged and failed by tearing out from under the rivet heads at approximately $0.75c_e$ as a result of either a large local pressure difference across the elevator skin or local stress concentrations. (See fig. 29.) The external and internal pressures of the elevator were therefore measured to determine whether a local aerodynamic condition was causing the failure.

Two pressure belts were used to measure the external pressures on the upper surface. One belt was located at station 47 and a small belt at the station of failure (station 50). No appreciable differences were noted, however, in the external pressures at stations 47 and 50, and only the pressures at station 47 are shown in

figure 30. This figure shows no irregular or excessive external pressures in the area of failure ($0.75c_e$) at M = 0.20. Additional tests made at M = 0.35 and 0.45 showed similar results and the bulge was therefore concluded to be a result of a local structural weakness.

The possibility of venting the elevator in order to nullify the pressure drop across the skin and thus to eliminate the skin deflection was investigated. It was necessary to determine the internal pressure of the elevator before attempting to choose a vent location. Figure 31 presents the effect of elevator angle on the internal pressure coefficient P_i at α = 0° and M = 0.20. The internal pressure was measured with normal leakage into the elevator and with all apparent openings such as the elevator hinge pockets sealed. A comparison of figures 30 and 31 shows that the normal elevator leakage provides probably the highest negative internal pressure and therefore the lowest pressure difference across the elevator skin; thus air vents would be of no practical benefit. It must be concluded that structural loads cause local stress concentrations at the middle hinge pocket and result in failure of the skin at this location.

CONCLUSIONS

The following conclusions may be drawn from the investigation described in this report:

1. A large increase in hinge-moment parameter $C_{h\delta}$ (rate of change of hinge-moment coefficient with elevator deflection) occurred for the metal elevator as the Mach number M was increased. The low-speed value of -0.0015 at M = 0.20 increased to -0.0032 at M = 0.70. The hinge-moment parameter $C_{h\alpha}$ (rate of change of hinge-moment coefficient with angle of attack) changed from 0.0024 at M = 0.20 to 0.0027 at M = 0.70 with a minimum value of 0.0020 at M = 0.35.

2. The metal elevator effectiveness decreased with increasing speed. This effect is believed to be a result of the elevator gap being unsealed. The low-speed value of 0.51 at M = 0.020 decreased to 0.34 at M = 0.70.

3. The values of $C_{h_\delta} = -0.0015$ and $C_{h_\alpha} \approx 0$ desired for this tail surface when used on the airplane for which it was designed may be obtained by modifying the original elevator to have a modified blunt nose (elevator 3) and a cusped contour behind the hinge line (elevator 2).

4. The incremental changes in C_{h_δ} due to elevator nose-shape modifications were of about the same magnitude as would be predicted by the use of recently published methods.

5. Trailing-edge strips of $\frac{1}{8}$-inch diameter and 24 percent span length on the metal elevator reduced the value of $C_{h_\alpha} = 0.0020$ to zero, but with an accompanying increase in C_{h_δ} from -0.0015 to -0.0040 at $M = 0.35$. No appreciable loss of trailing-edge-strip effectiveness in changing C_{h_α} was apparent up to $M = 0.65$.

6. The region of laminar flow over the stabilizer was limited to approximately 10 percent of the stabilizer chord.

REFERENCES

1. Swanson, Robert S., and Toll, Thomas A.: Jet-Boundary
     Corrections for Reflection-Plane Models in Rectan-
     gular Wind Tunnels. NACA ARR No. 3E22, 1943.

2. Schueller, Carl F., and Korycinski, Peter F.: Effect
     of Fabric Deflection at High Speeds on the Aero-
     dynamic Characteristics of the Horizontal Tail
     Surface of an SB2D-1 Airplane. NACA ARR No. L5F10a,
     1945.

3. Glauert, H.: Theoretical Relationships for an Aero-
     foil with Hinged Flap. R. & M. No. 1095, British
     A.R.C., 1927.

4. Sears, Richard I.: Wind-Tunnel Data on the Aerody-
     namic Characteristics of Airplane Control Surfaces.
     NACA ACR No. 3L08, 1943.

5. Perring, W. G. A.: The Theoretical Relationships for
     an Aerofoil with a Multiply Hinged Flap System.
     R. & M. No. 1171, British A.R.C., 1928.

6. Goett, Harry J., and Reeder, J. P.: Effects of Ele-
     vator Nose Shape, Gap, Balance, and Tabs on the
     Aerodynamic Characteristics of a Horizontal Tail
     Surface. NACA Rep. No. 675, 1939.

7. Purser, Paul E., and Riebe, John M.: Wind-Tunnel
     Investigation of Control-Surface Characteristics.
     XV - Various Contour Modifications of a 0.30-
     Airfoil-Chord Plain Flap on an NACA 66(215)-014 Air-
     foil. NACA ACR No. 3L20, 1943.

8. Purser, Paul E., and Toll, Thomas A.: Analysis of
     Available Data on Control Surfaces Having Plain-
     Overhang and Frise Balances. NACA ACR No. L4E13,
     1944.

TABLE I

PHYSICAL CHARACTERISTICS OF THE HORIZONTAL TAIL SURFACE

$$c$$

$$c_b = 0.48c_e \qquad c_e = 0.28c$$
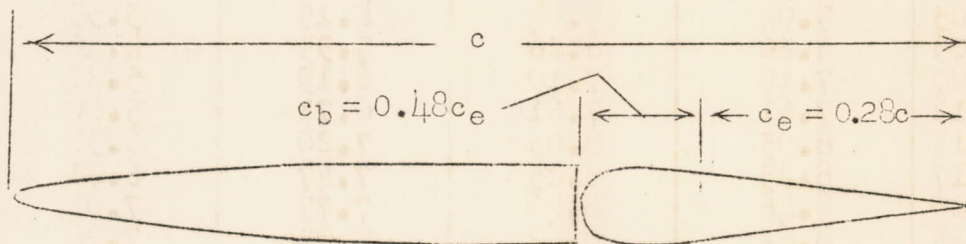
Airfoil section . . . . Modified NACA 66-009
Semispan, $b/2$, in. 112.0
Root chord, c_r, in. 66.0
Tip chord, c_t, in. 33.0
Area of semispan, $S_w/2$, sq in. 5275.0
Mean aerodynamic chord, in. 51.3
Aspect ratio, A 4.76
Taper ratio 0.50
Area of stabilizer, S_s, sq in. 3259.0
Area of elevator, S_e, sq in. 1429.0
Area of overhang, S_b, sq in. 596.0
Root-mean-square elevator chord behind hinge
    line, $\bar{c}_e$, in. 13.74
Elevator overhang, c_b/c_e 0.48

NATIONAL ADVISORY
COMMITTEE FOR AERONAUTICS

TABLE II

COORDINATES FOR WOODEN ELEVATORS IN PERCENT CHORD

x	Elevator 1 y	Elevator 2 y	Elevator 3 y	Elevator 4 y
0	0	0	0	0
.51	3.91	3.91	3.19	2.47
1.03	5.04	5.04	4.19	3.33
2.06	6.26	6.26	5.33	4.40
3.09	7.10	7.10	6.19	5.27
4.12	7.61	7.61	6.71	5.80
5.14	8.03	8.03	7.20	6.38
6.17	8.23	8.23	7.47	6.71
7.20	8.46	8.46	7.75	7.04
8.23	8.62	8.62	7.95	7.28
9.26	8.75	8.75	8.16	7.57
10.29	8.85	8.85	8.31	7.78
11.32	8.91	8.91	8.43	7.94
12.35	8.93	8.93	8.50	8.07
13.37	8.95	8.95	8.59	8.23
14.40	8.99	8.99	8.63	8.27
16.46	8.95	8.95	8.69	8.44
18.52	8.87	8.87	8.65	8.44
20.58	8.76	8.76	8.60	8.44
22.63	8.64	8.64	8.54	8.44
24.69	8.44	8.44	8.38	8.31
28.81	8.03	8.03	8.01	7.99
32.92	7.57	7.57	7.55	7.53
37.04	(a)	7.10	7.10	7.10
41.15		6.59	6.59	6.59
45.27		6.13	6.13	6.13
49.38		5.58	5.58	5.58
53.50		5.04	5.04	5.04
57.61		4.53	4.53	4.53
61.73		3.93	3.93	3.93
65.84		3.48	3.48	3.48
69.96		3.01	3.01	3.01
74.08		2.47	2.47	2.47
78.19		2.02	2.02	2.02
82.31		1.56	1.56	1.56
86.42		1.13	1.13	1.13
90.54		.82	.82	.82
94.65		.52	.52	.52
98.77	↓	.27	.27	.27

Trailing-edge radius = 0.05 inch

(a)Straight taper behind 32.4 percent chord.
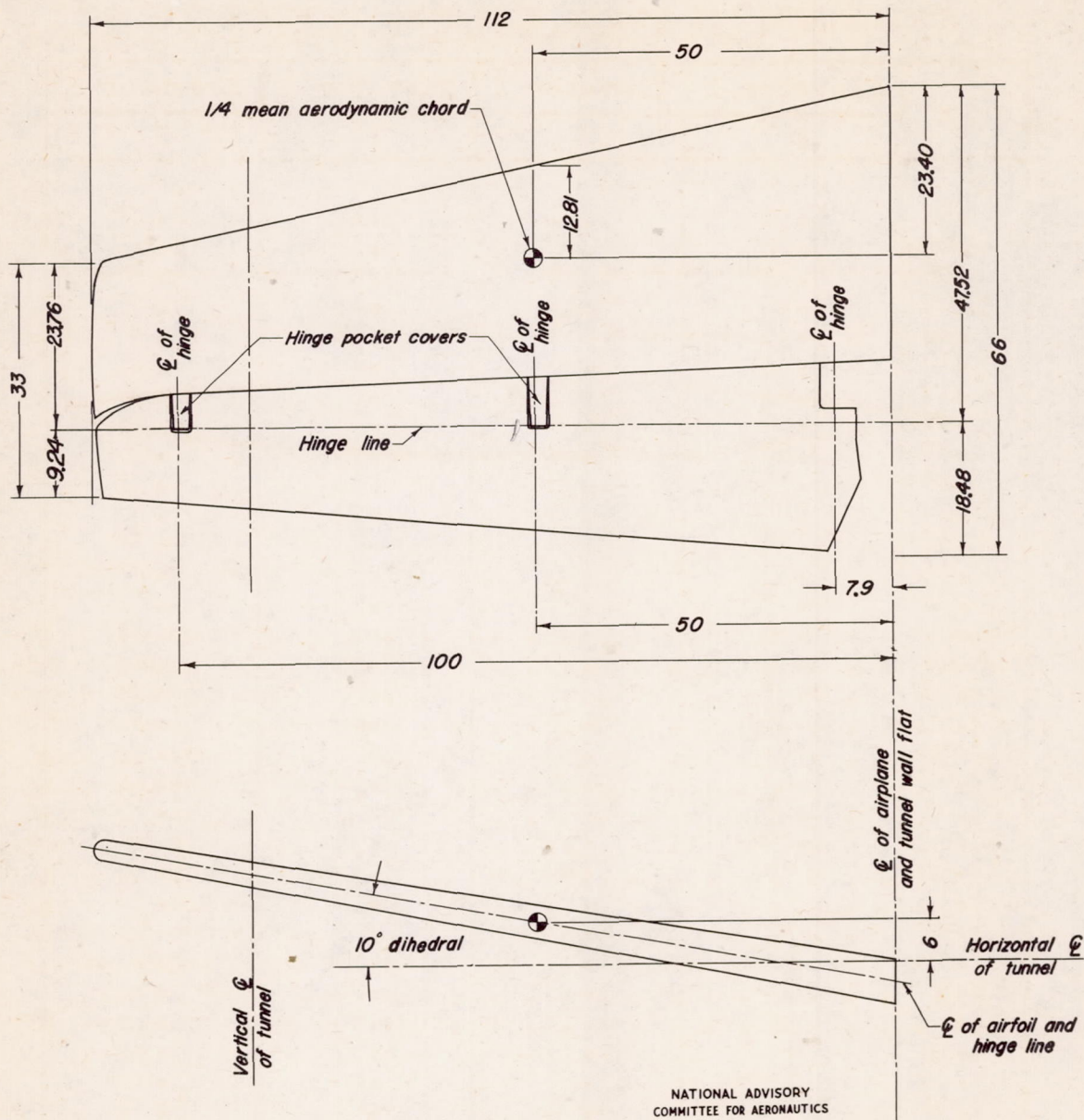
Figure 1.— General arrangement of the horizontal tail surface in the Langley 16-foot high-speed tunnel. All dimensions shown are in inches and are measured in the plane of the section.
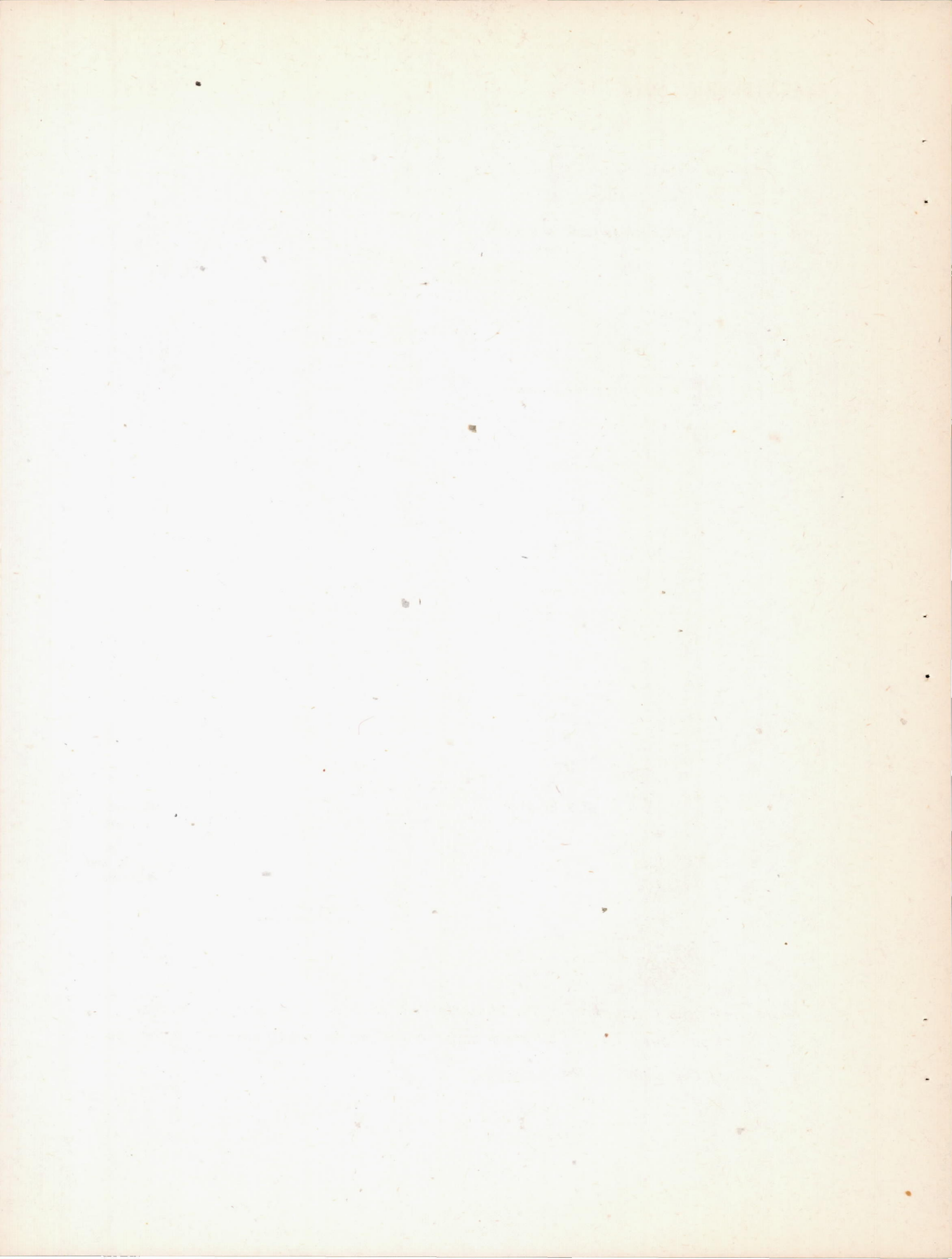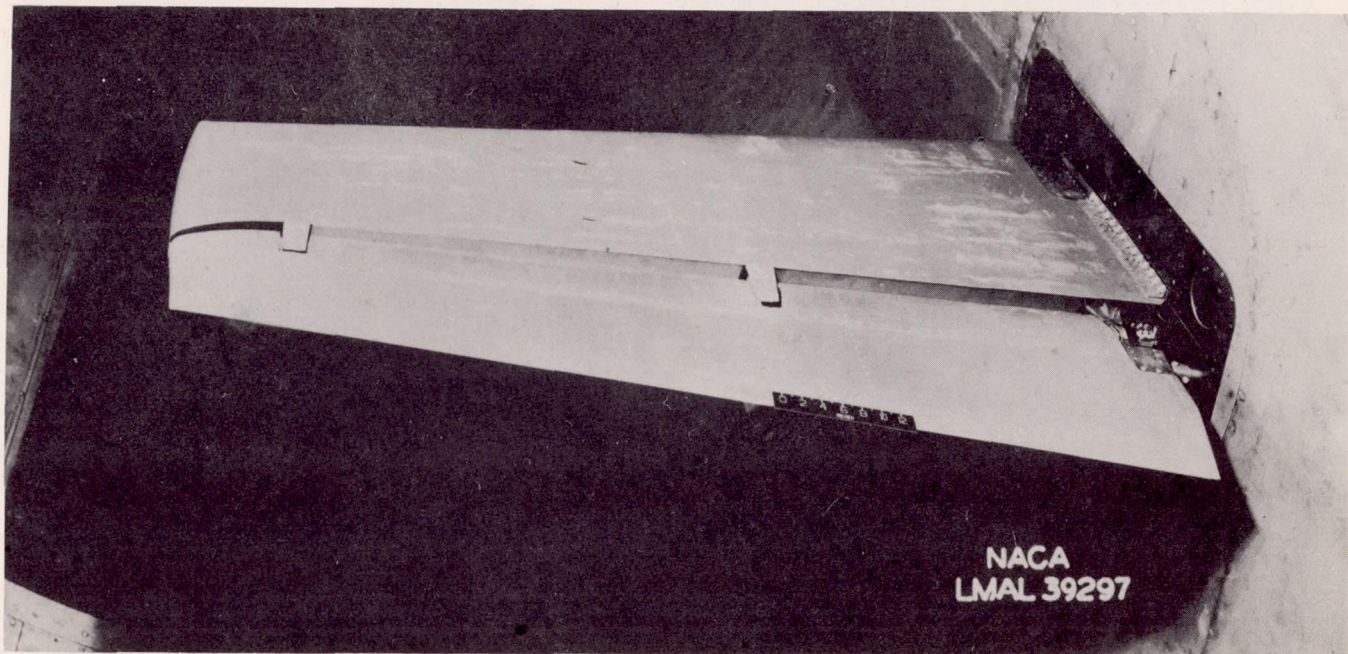
Figure 2.- General view of the semispan horizontal tail installed in
the Langley 16-foot high-speed tunnel.

Fig. 2

Nose shape   Elevator

Blunt

Modified blunt   3

Semielliptical   4
Original

ϕ
(deg)   Elevator

13   Original

7   2
3
4

Hinge point

Trailing — edge angle

Figure 3.— Contours of original metal elevator and elevators I to 4.

Fig. 3

Fig. 4

- Quarter span
- Half span
- Full span

Elevator skin

Linen tape

Tubing
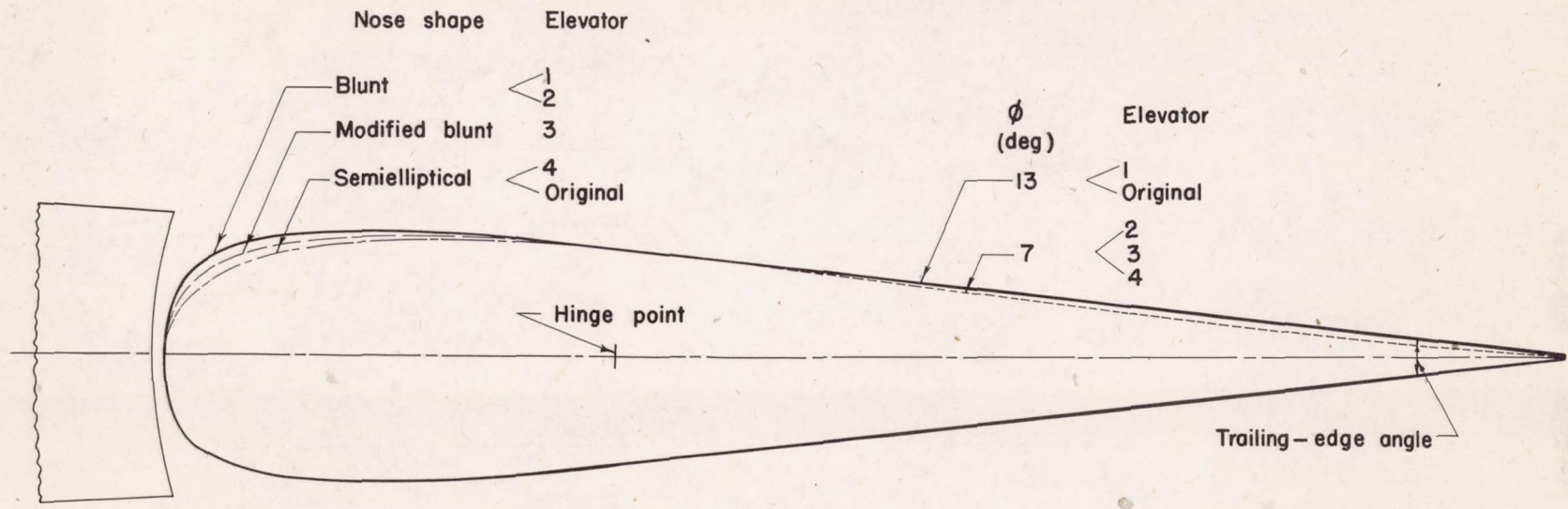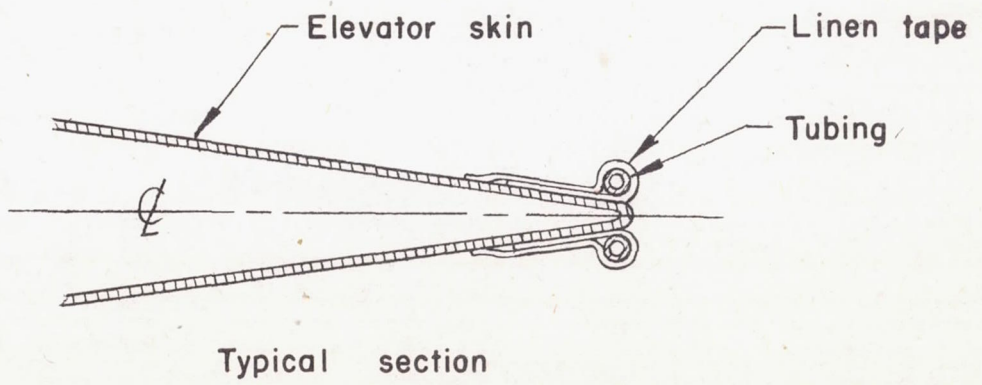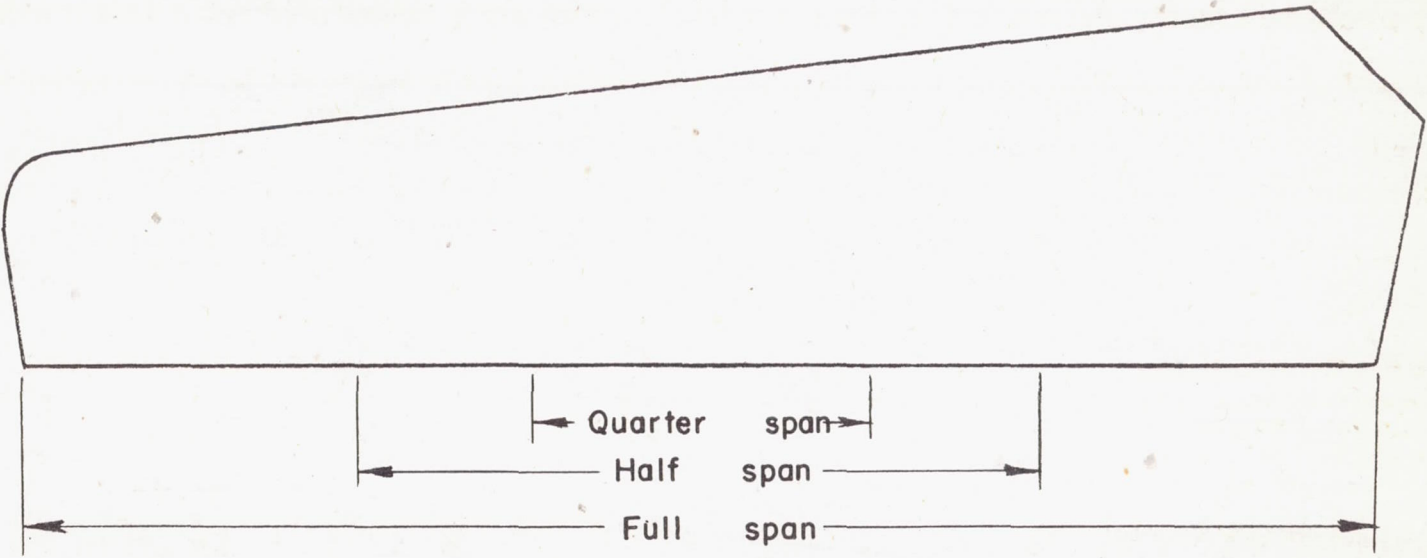
Typical section

NATIONAL ADVISORY
COMMITTEE FOR AERONAUTICS

Figure 4 .— Location and installation of trailing—edge strips on metal elevator.
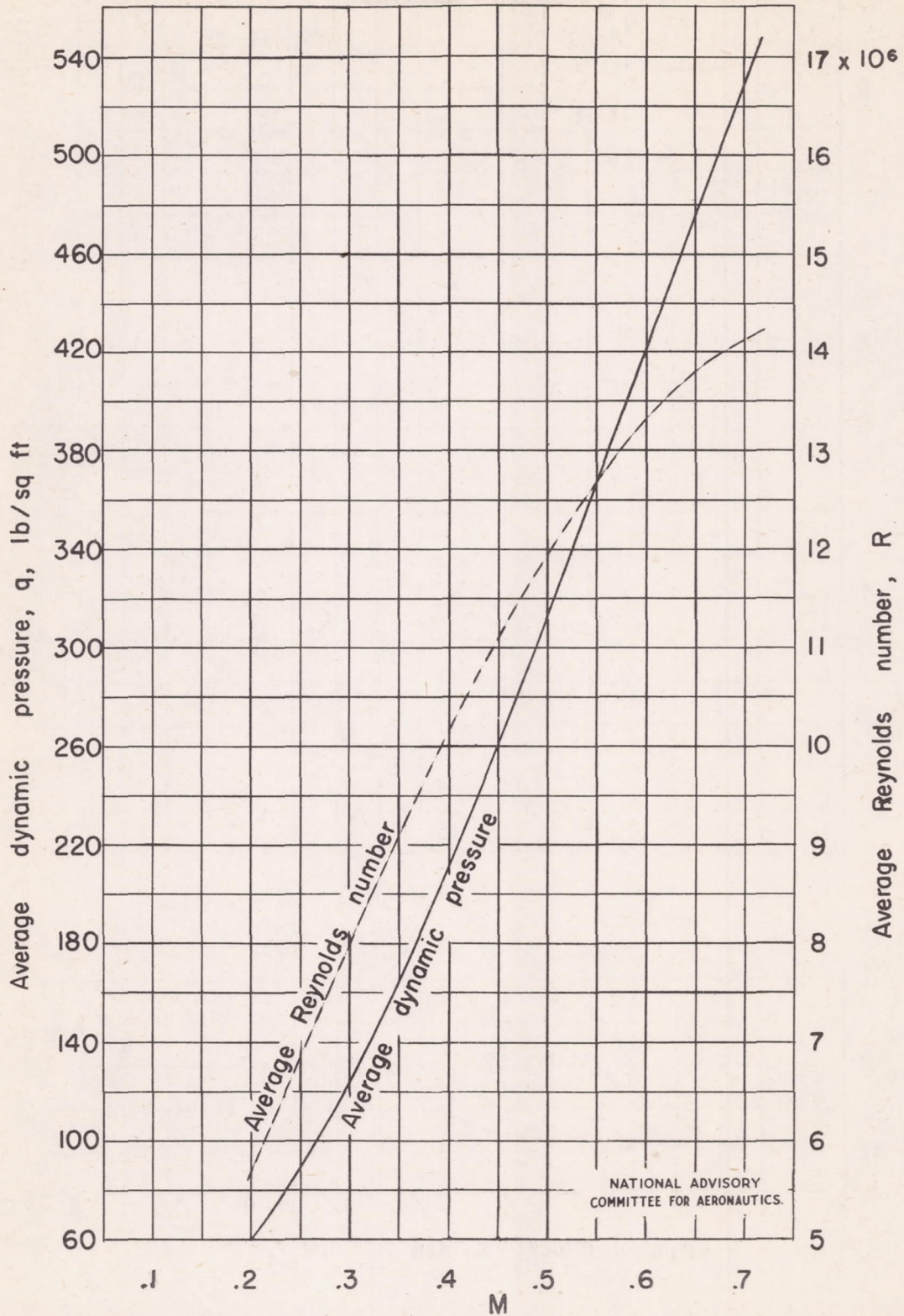
Figure 5. —— Variation of the average dynamic pressure
and average Reynolds number with test Mach number.

Fig. 6   NACA TN No. 1074
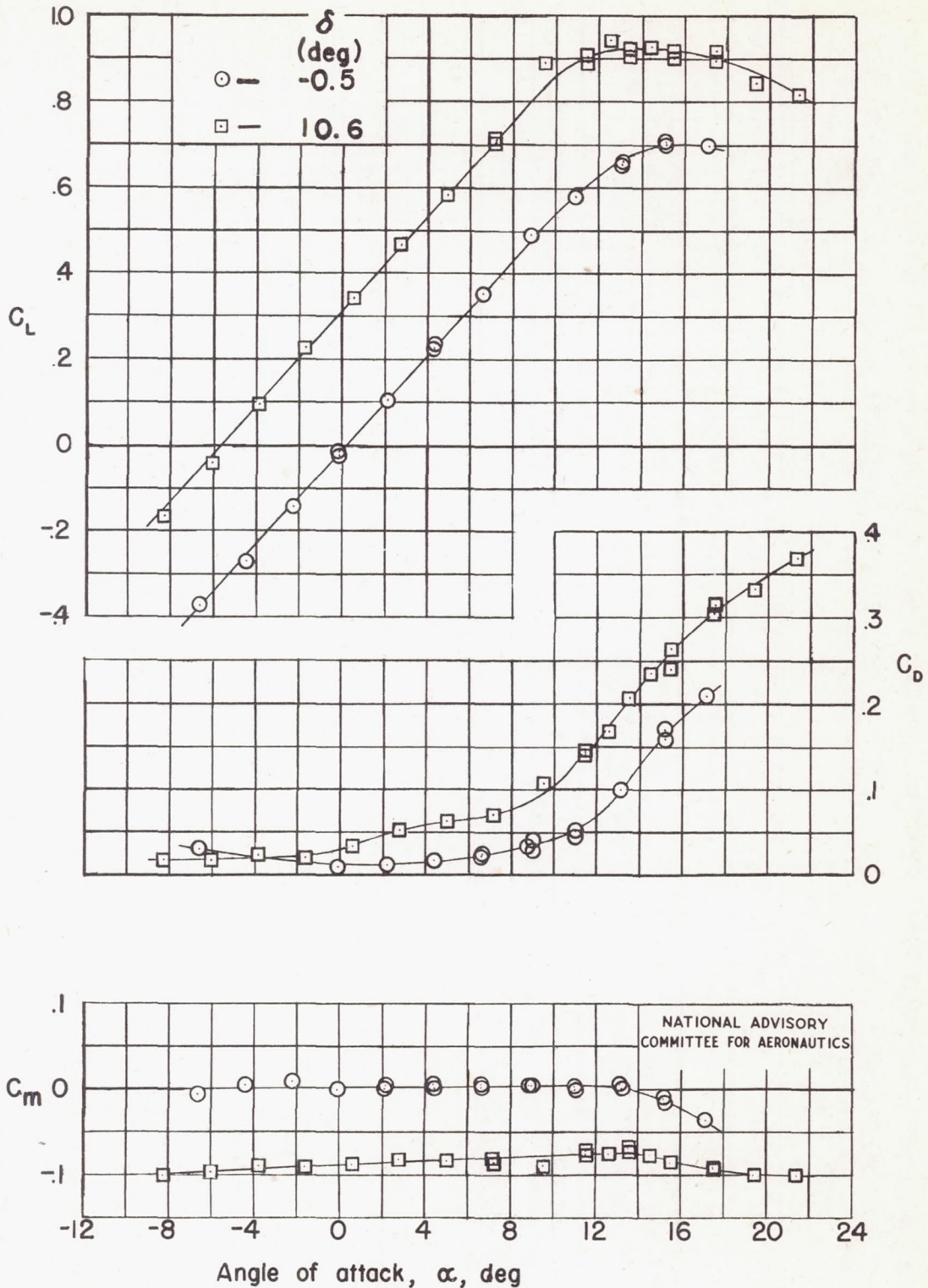
Figure 6.— Basic aerodynamic characteristics for two elevator angles. δ = -.5° and 10.6°; M=0.20.
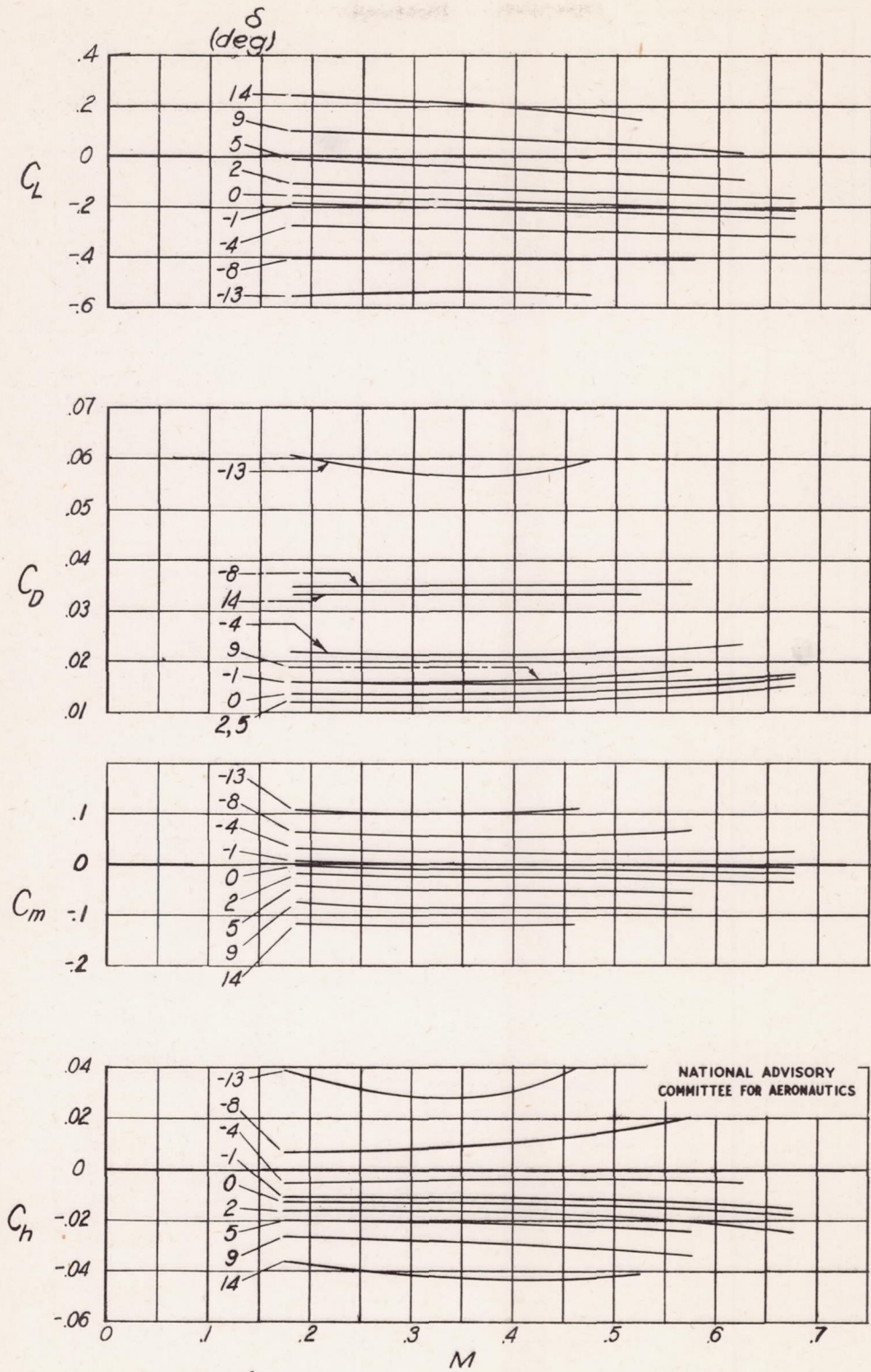
(a) α = -3°.

Figure 7.- Variation of aerodynamic characteristics with Mach number.
        Metal elevator.
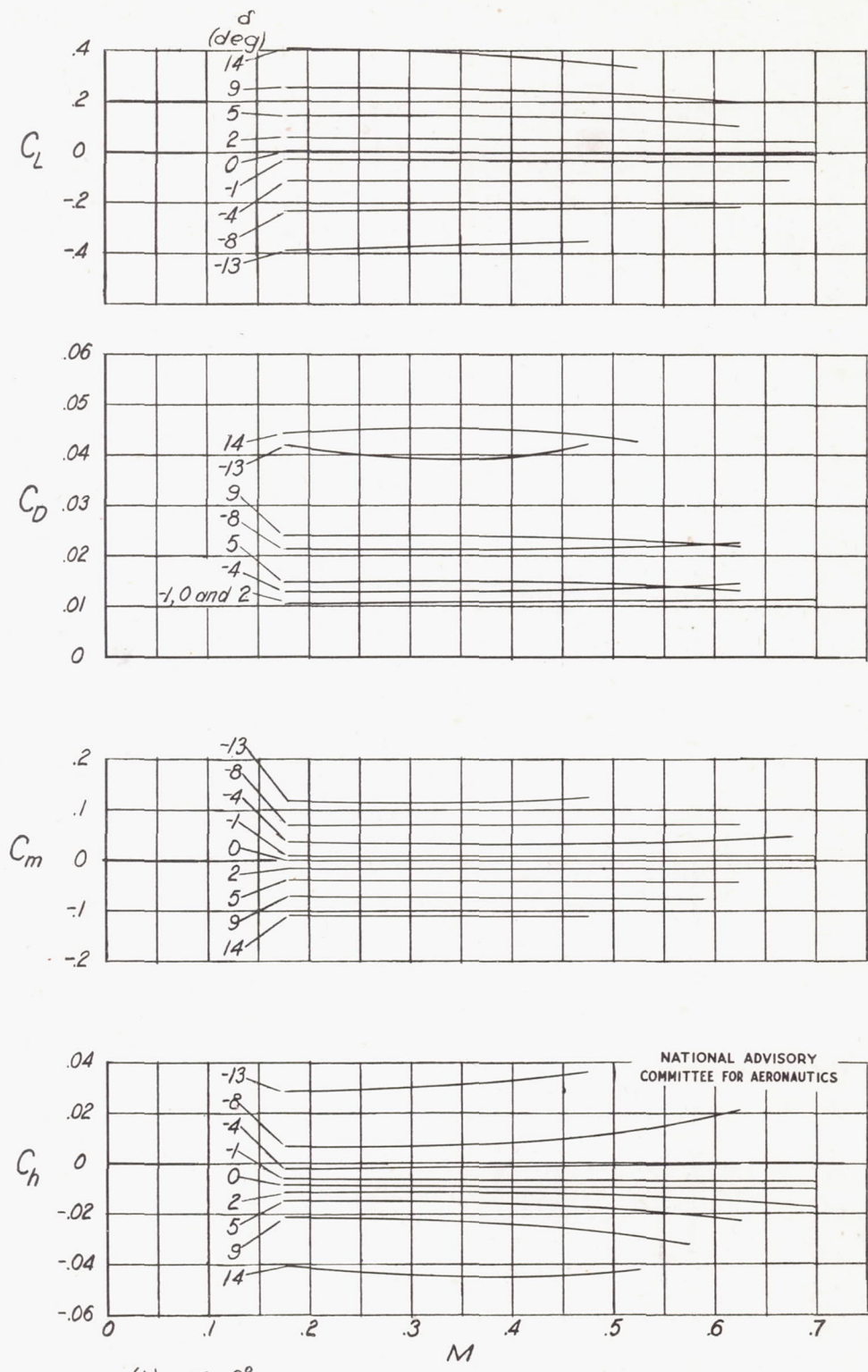
(b) $\alpha = 0.^\circ$

Figure 7.- Continued.

(c) $\alpha = 3°$.
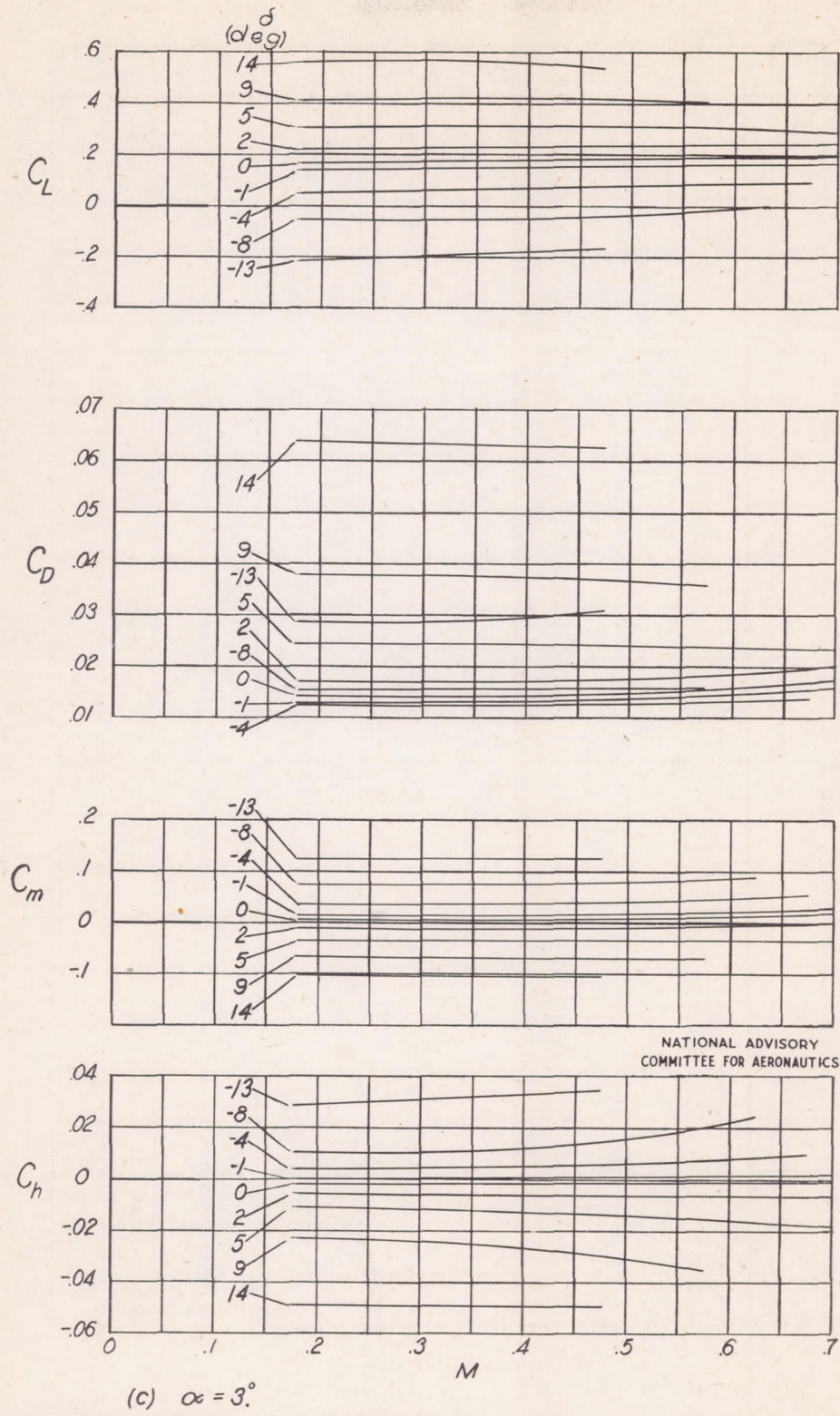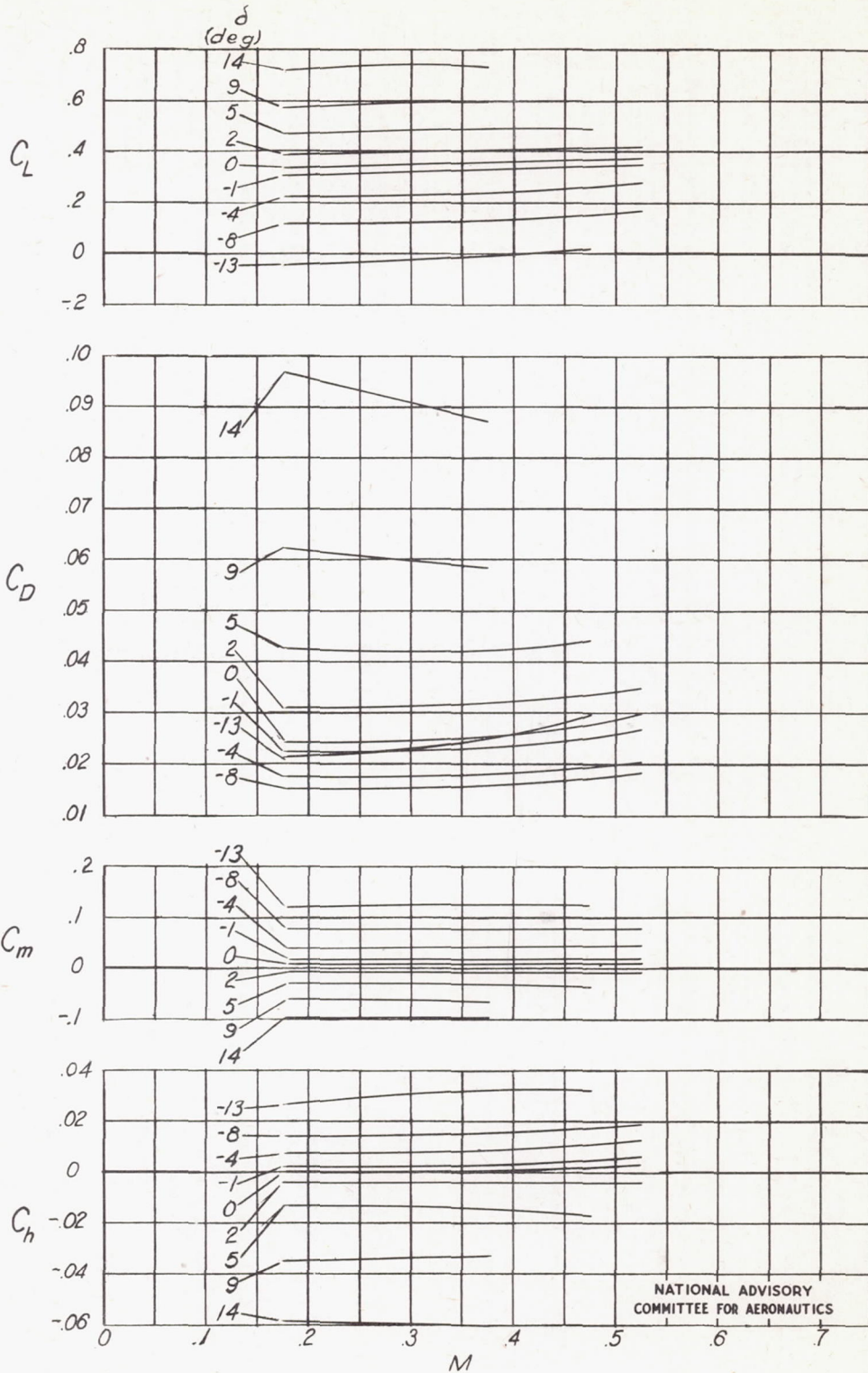
Figure 7.- Continued.

(d) $\alpha = 6°$.

Figure 7 .- Continued.

(e) $\alpha = 9°$.
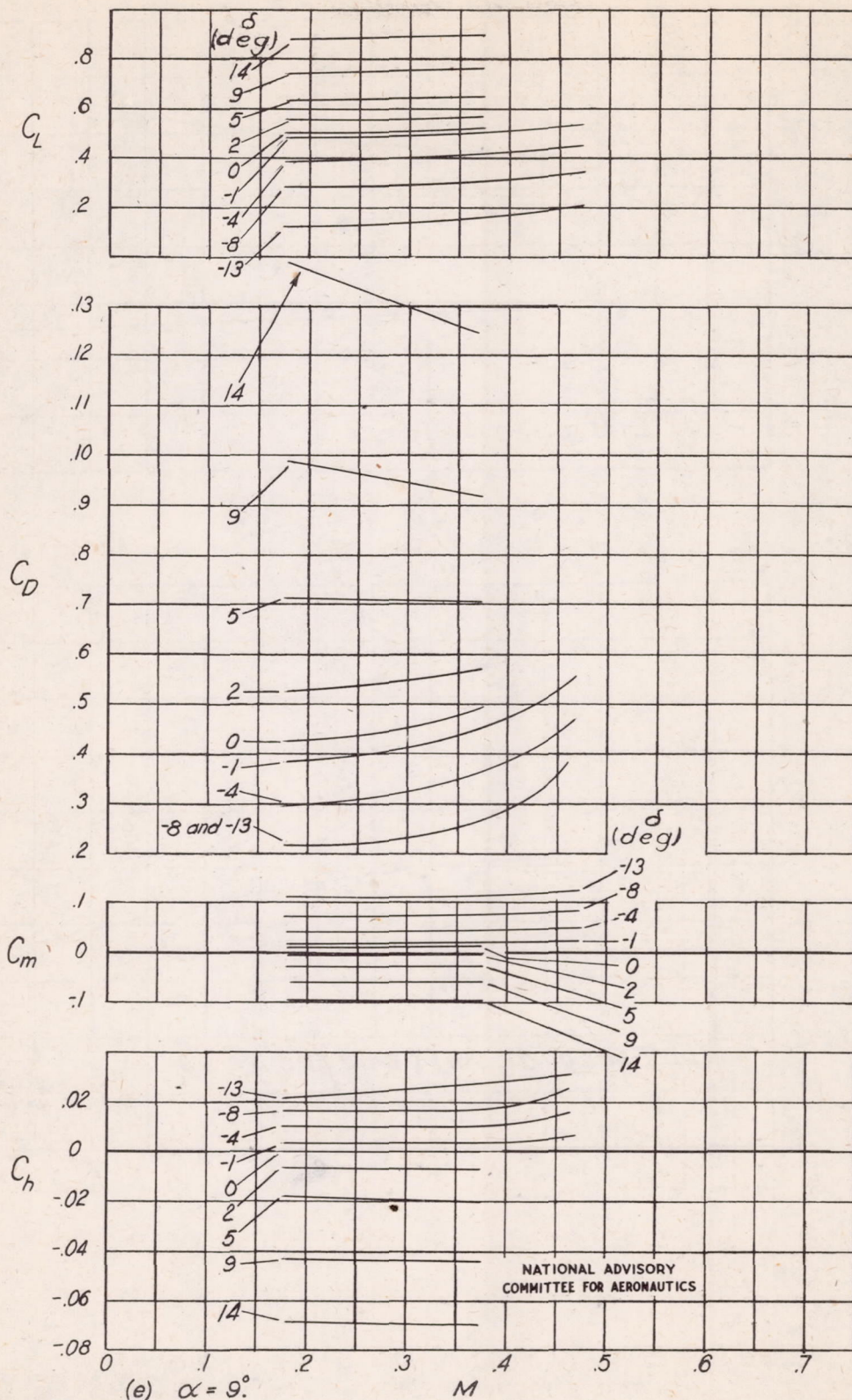
Figure 7.- Concluded.

Fig. 8

NACA TN No. 1074
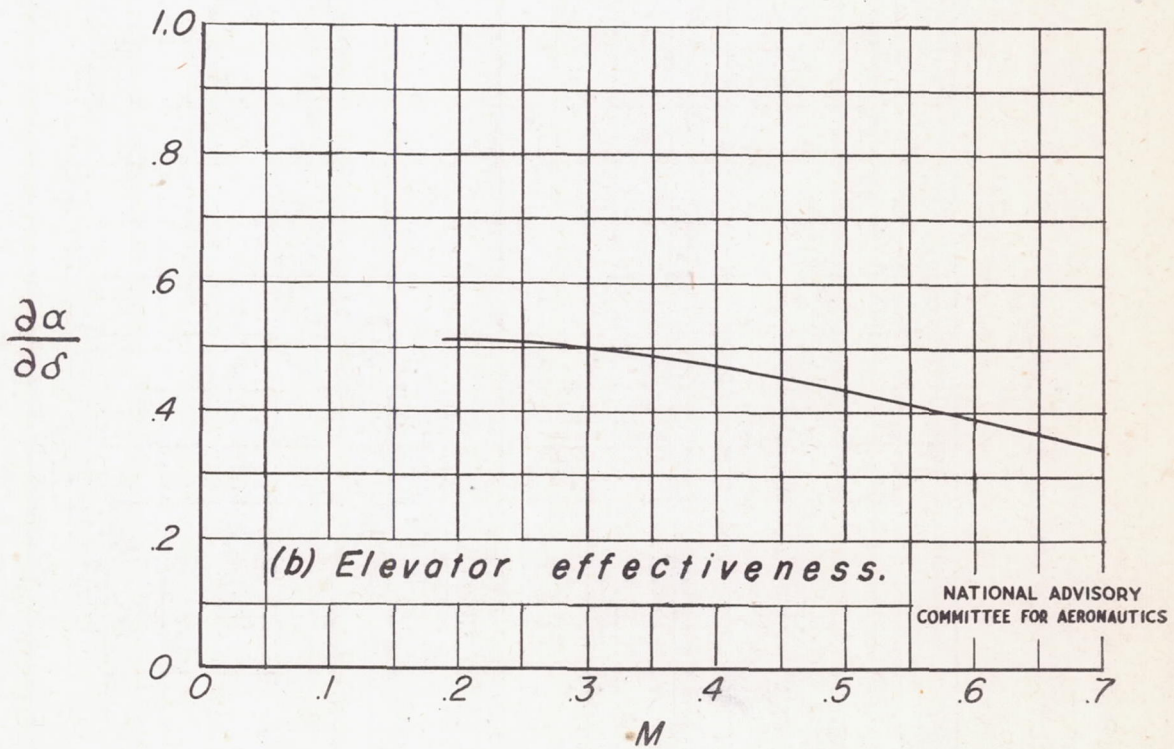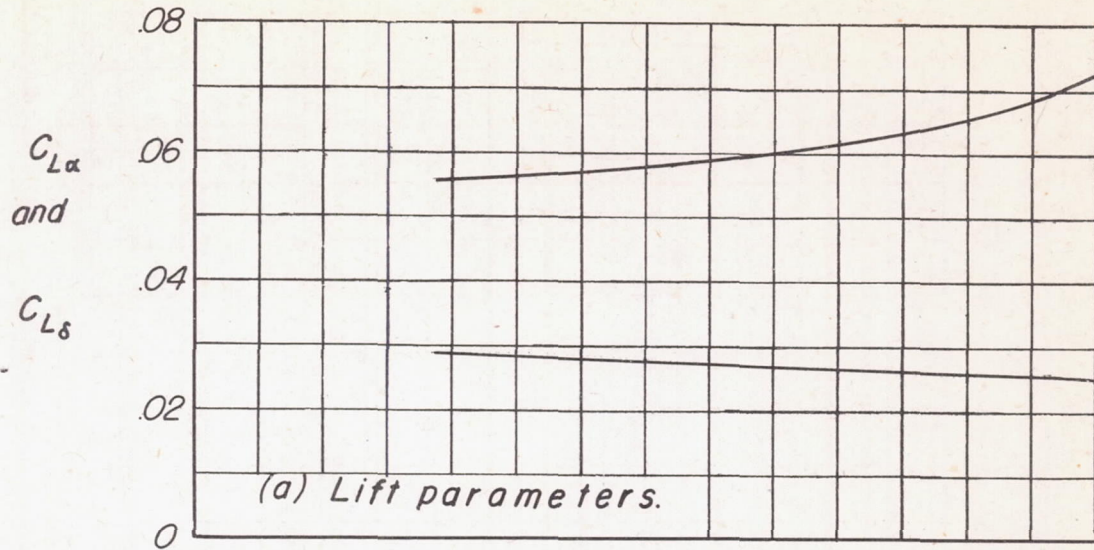
Figure 8 .— Effect of Mach number on lift parameters and elevator effectiveness.
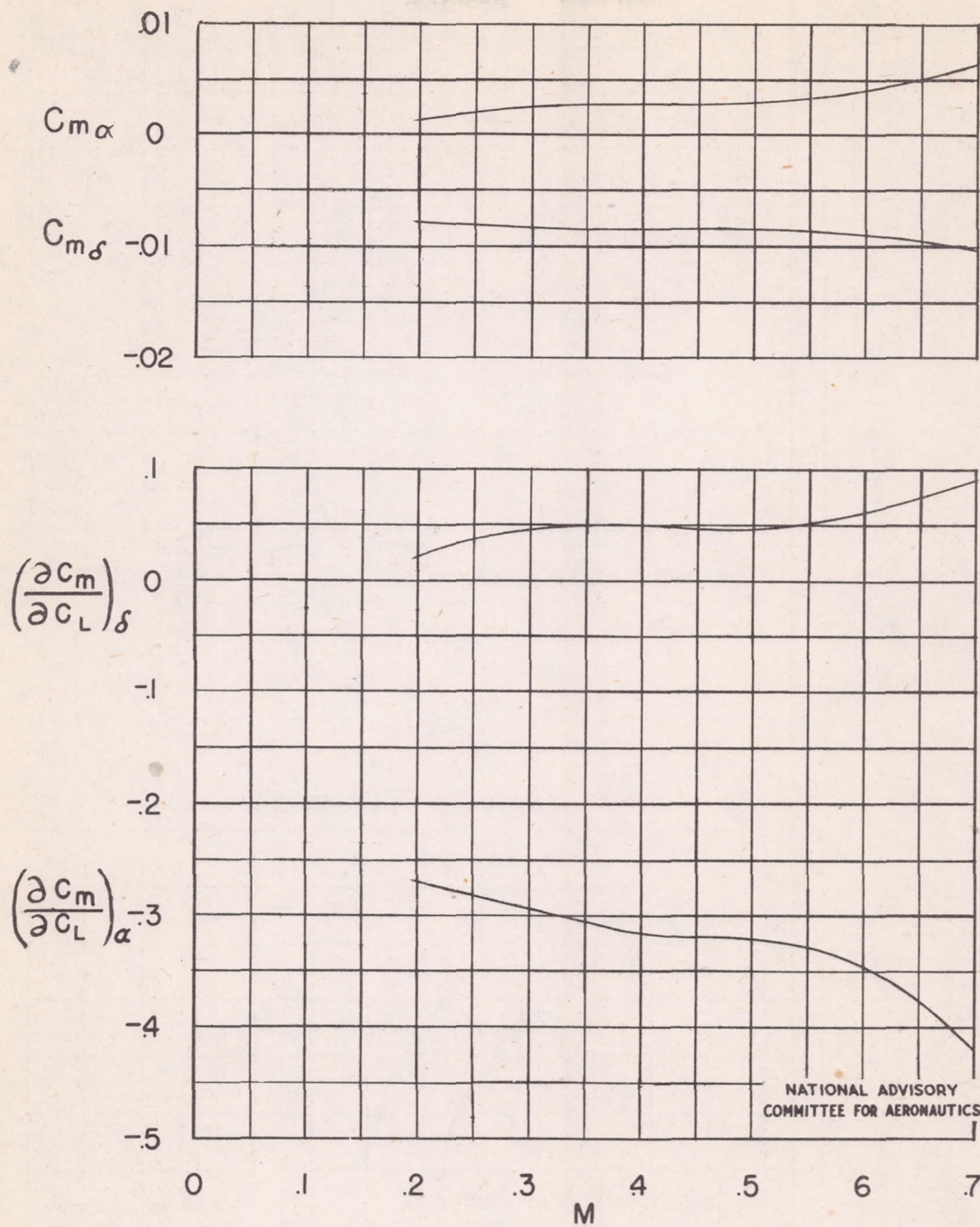
Figure 9 .— Variation of the pitching-moment-coefficient parameters
with Mach number. Metal elevator.

Fig. 10   NACA TN No. 1074
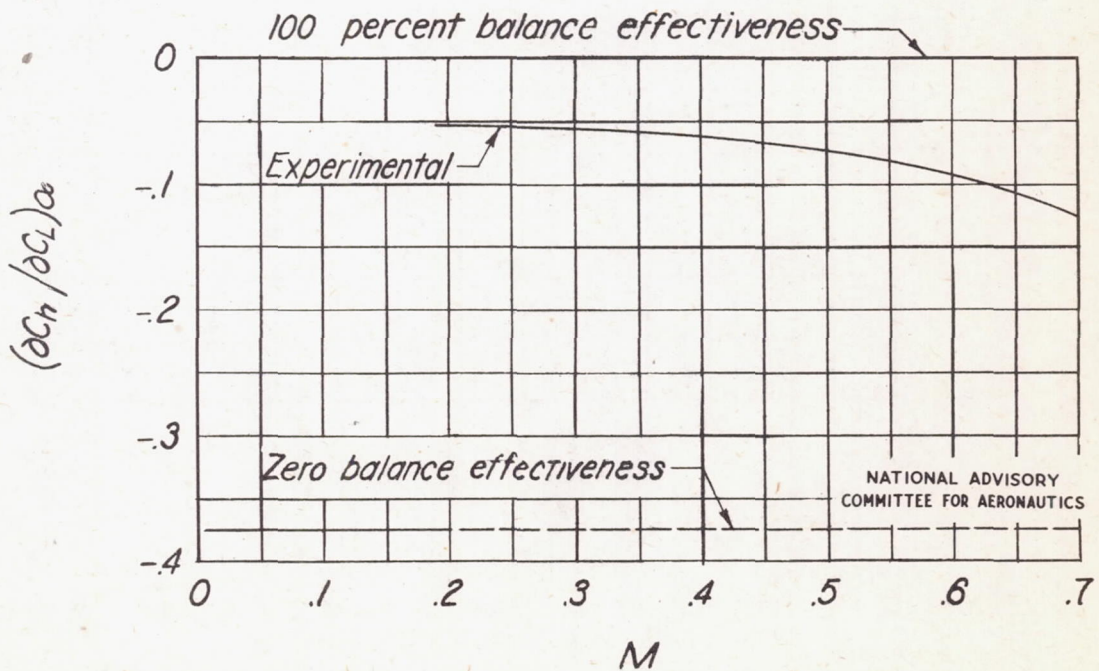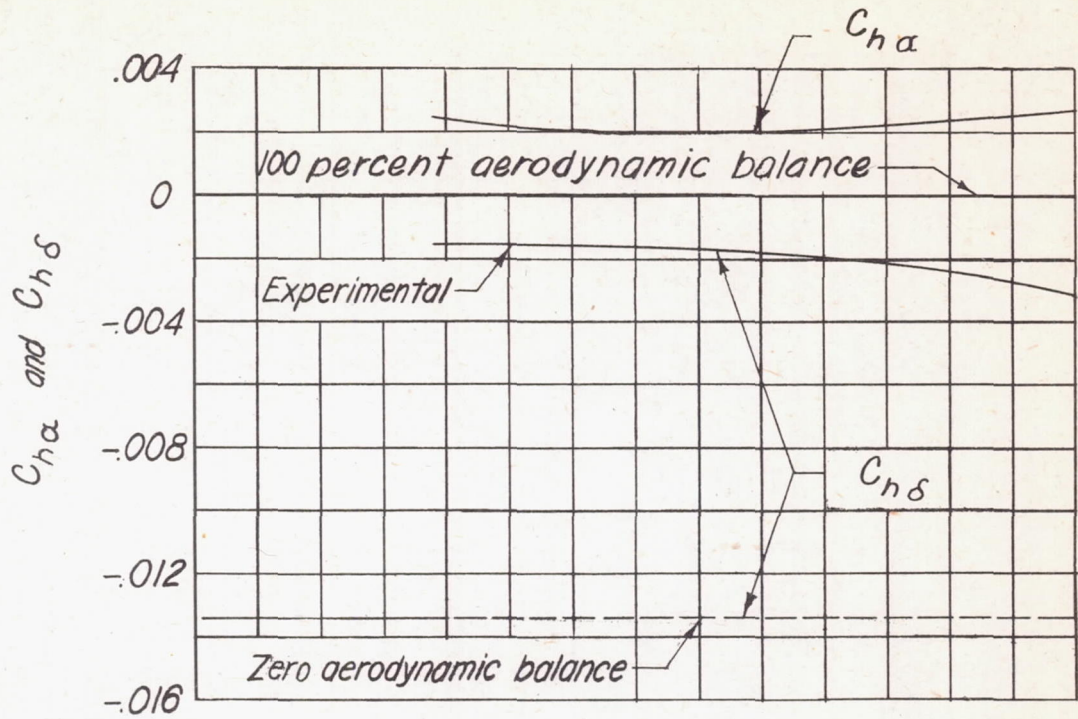
Figure 10.- The variation of the hinge-moment parameters with Mach
number. Metal elevator.

Figure 11. — Effect of elevator trailing-edge angle on elevator hinge-
moment coefficient. M= 0.35.
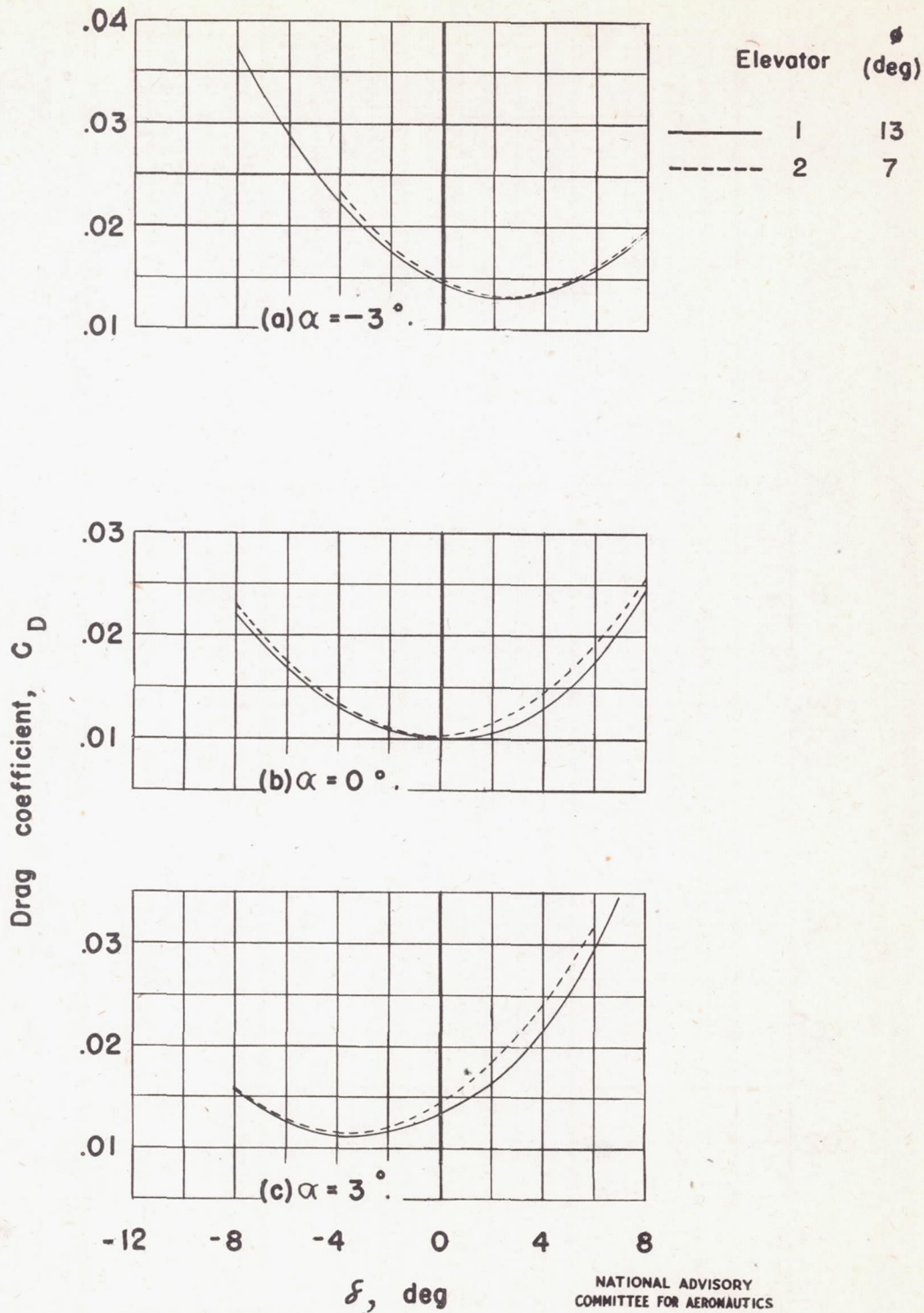
Figure 12.— Effect of elevator trailing-edge angle on drag coefficient. M = 0.35.
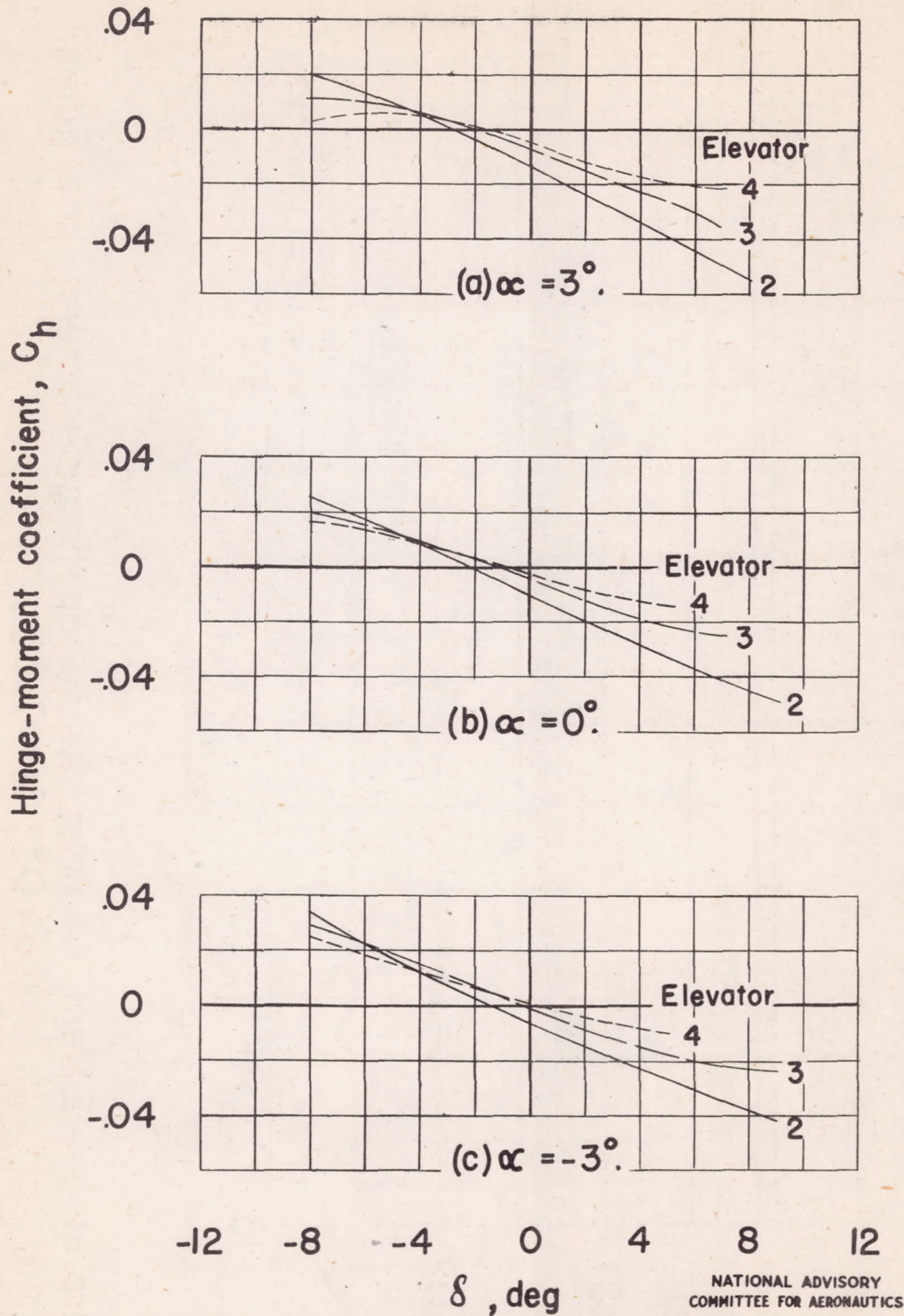
Figure 13.-Variation of hinge-moment coefficient with elevator angle for the three nose shapes. M= 0.35.

Fig. 14
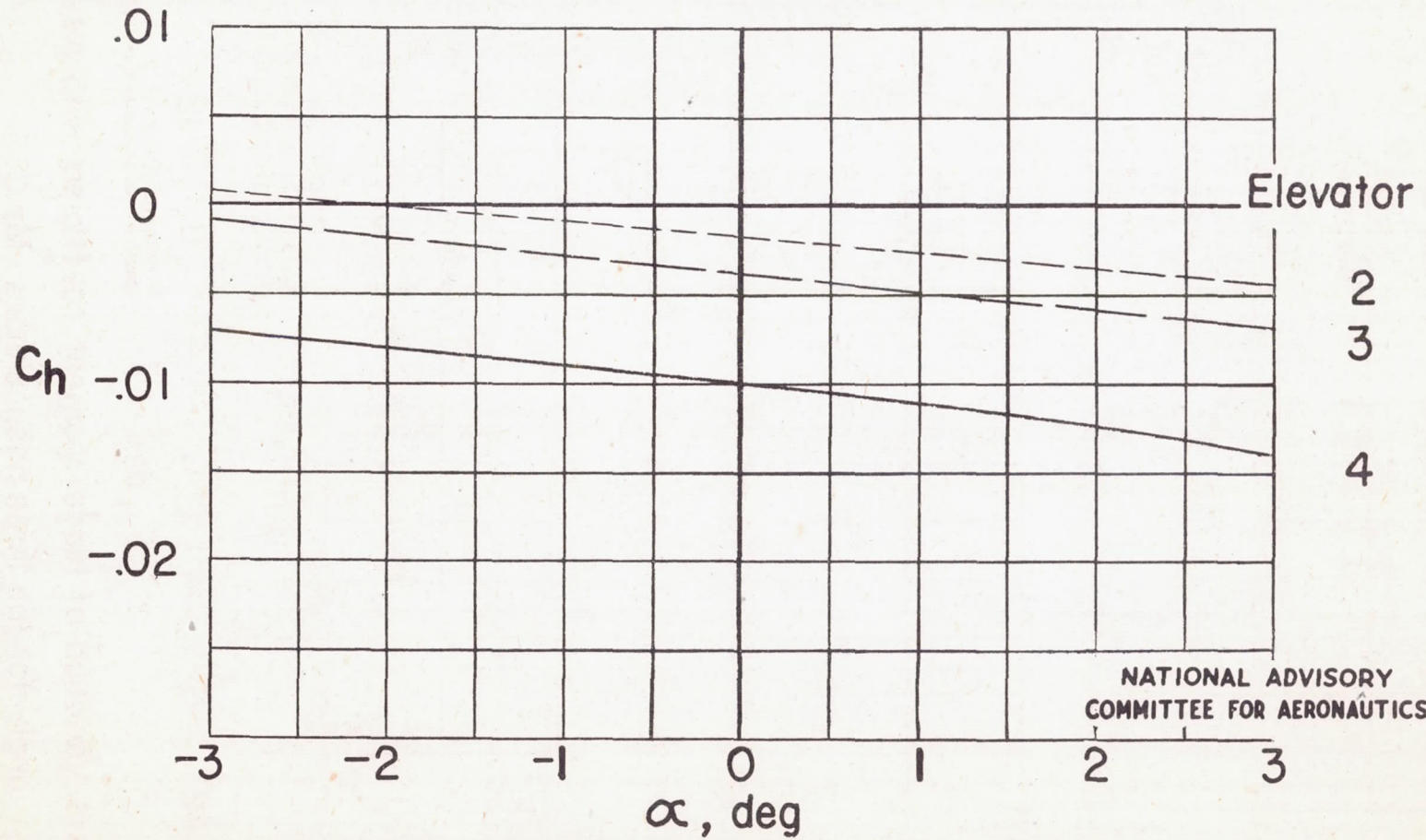
Figure 14 .— Effect of nose shape on hinge-moment coefficient. $\delta = 0°$; $M = 0.35$.
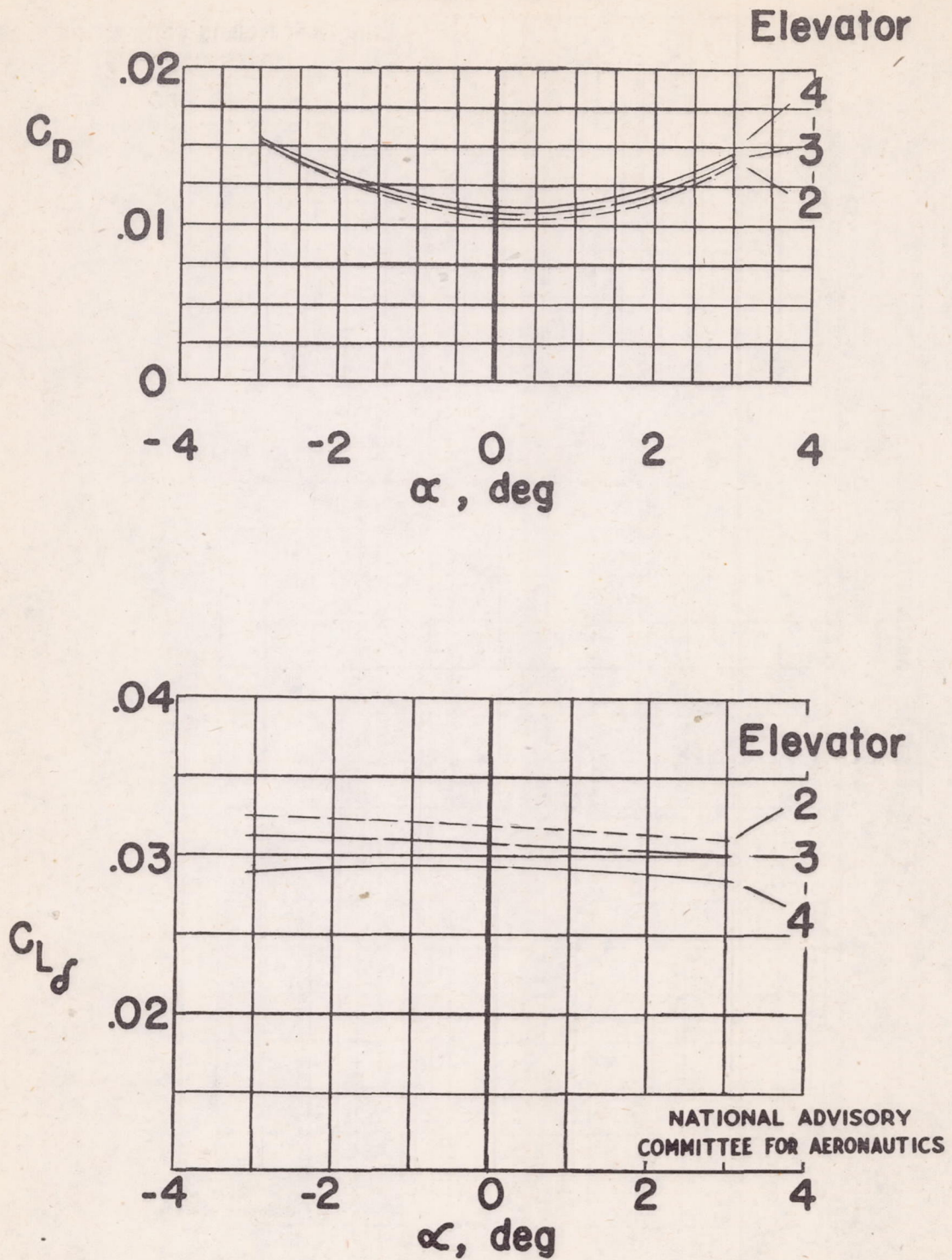
Figure 15.- Variation of C_D and C_{L_δ} with α for various nose shapes. $M = 0.35; \delta = 0°$.
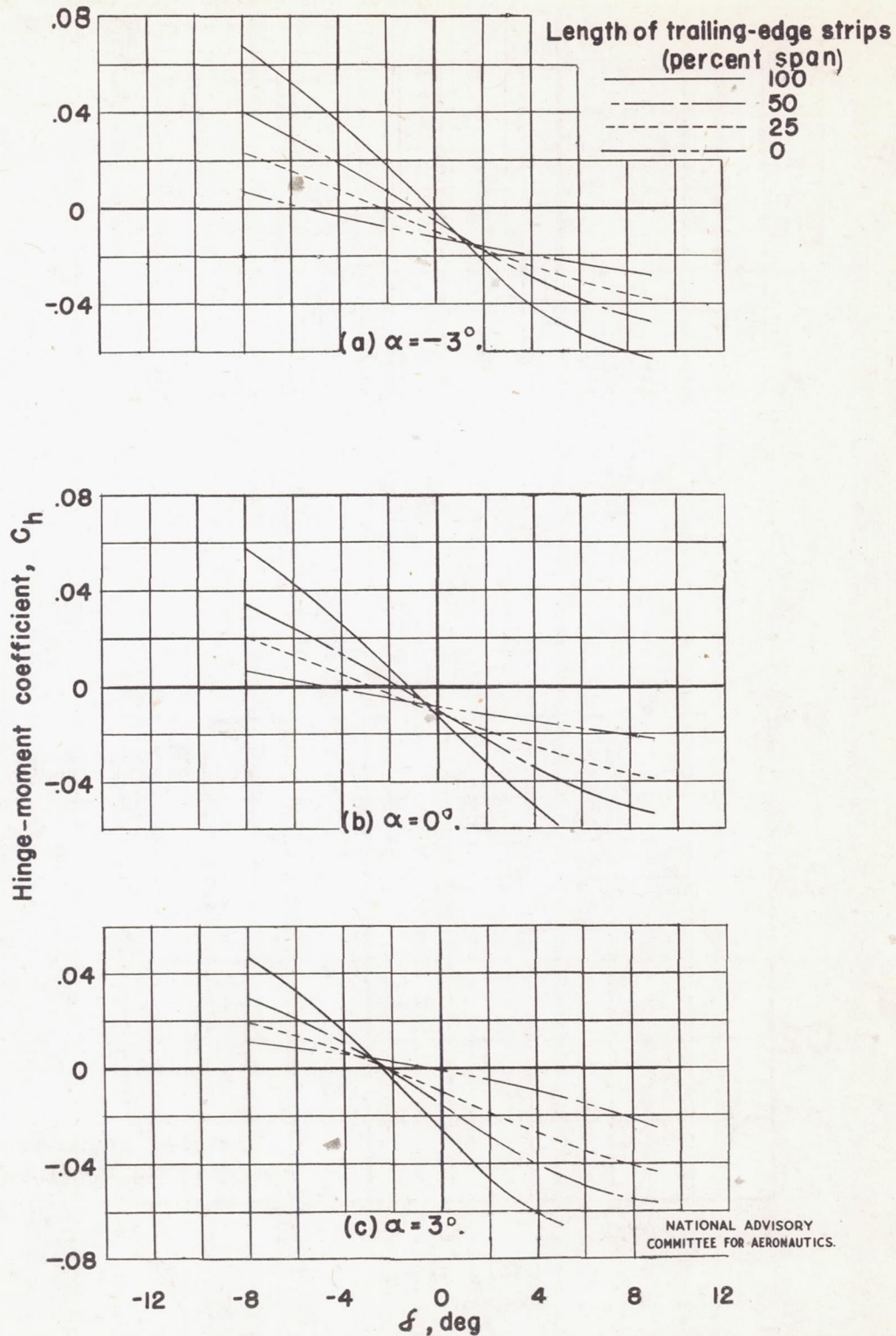
Figure 16.— Variation of C_h with elevator angle for four lengths of $\frac{1}{8}$-inch-diameter trailing-edge strips. M=0.35.
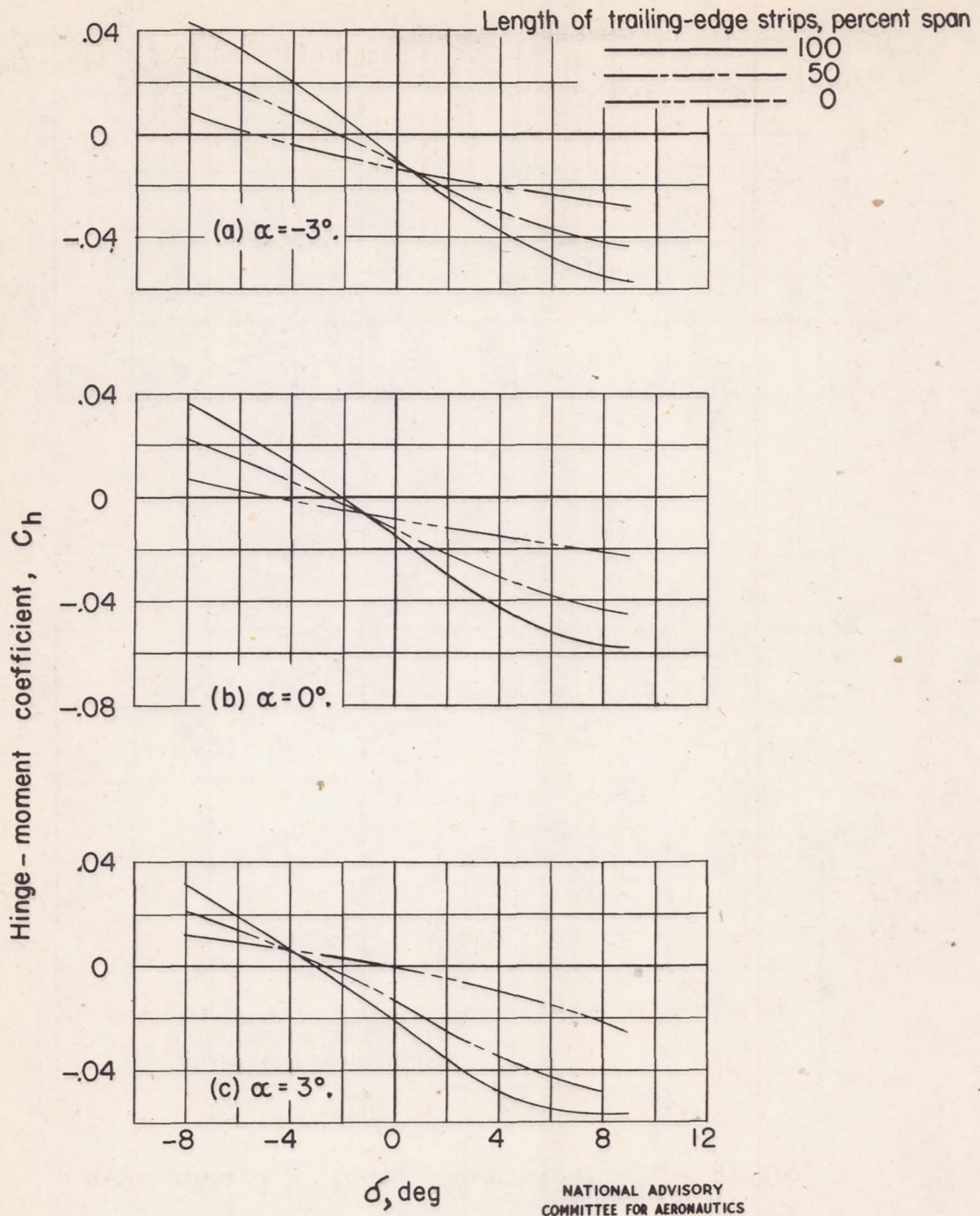
Figure 17.— Variation of C_h with elevator angle for three lengths of $\frac{1}{16}$-inch-diameter trailing-edge strips. M = 0.35.

Fig. 18   NACA TN No. 1074
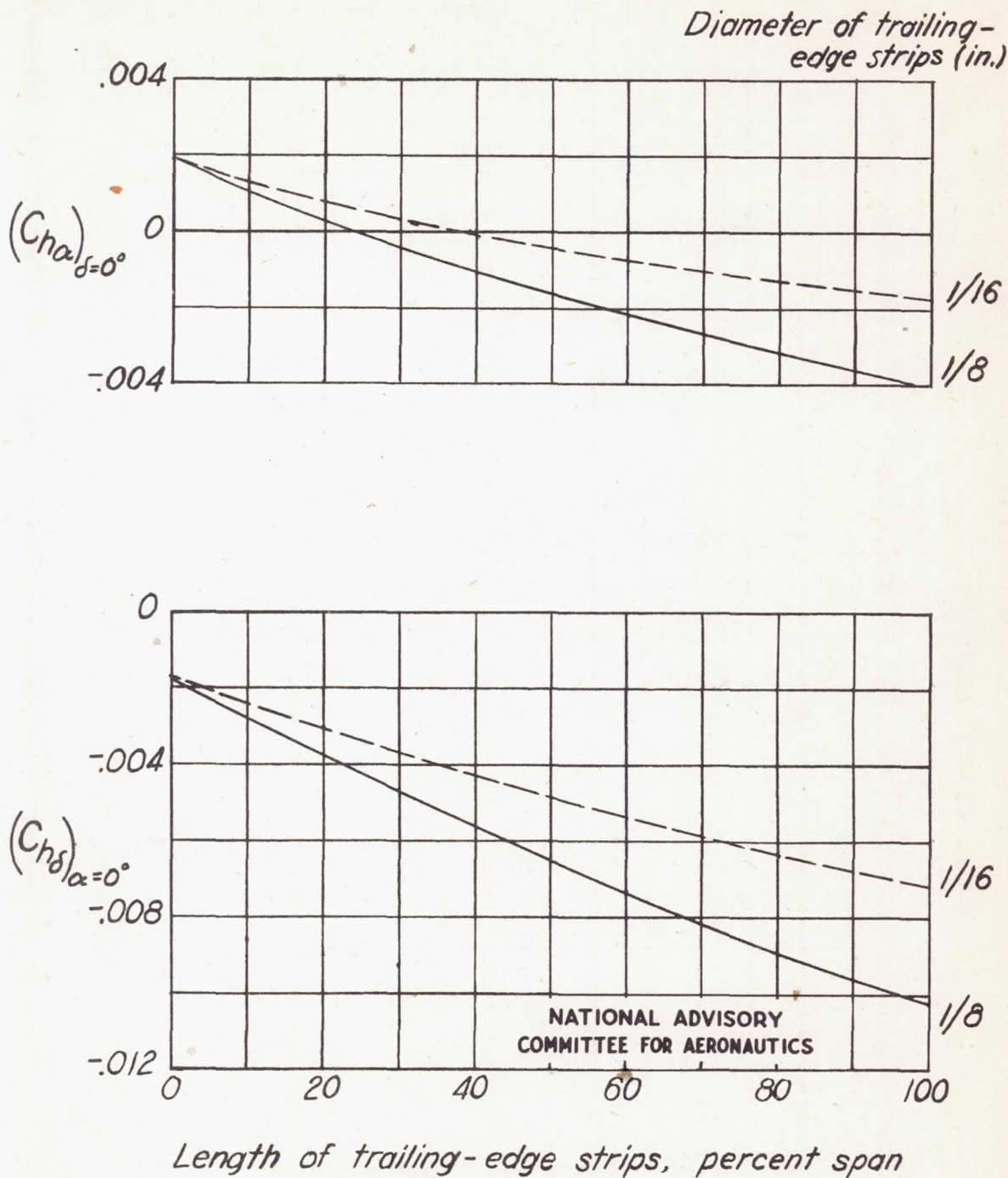
Figure 18.— Effect of length of trailing-edge strips of $\frac{1}{16}$-inch and $\frac{1}{8}$-inch diameter on $C_{h\alpha}$ and $C_{h\delta}$. M=0.35.
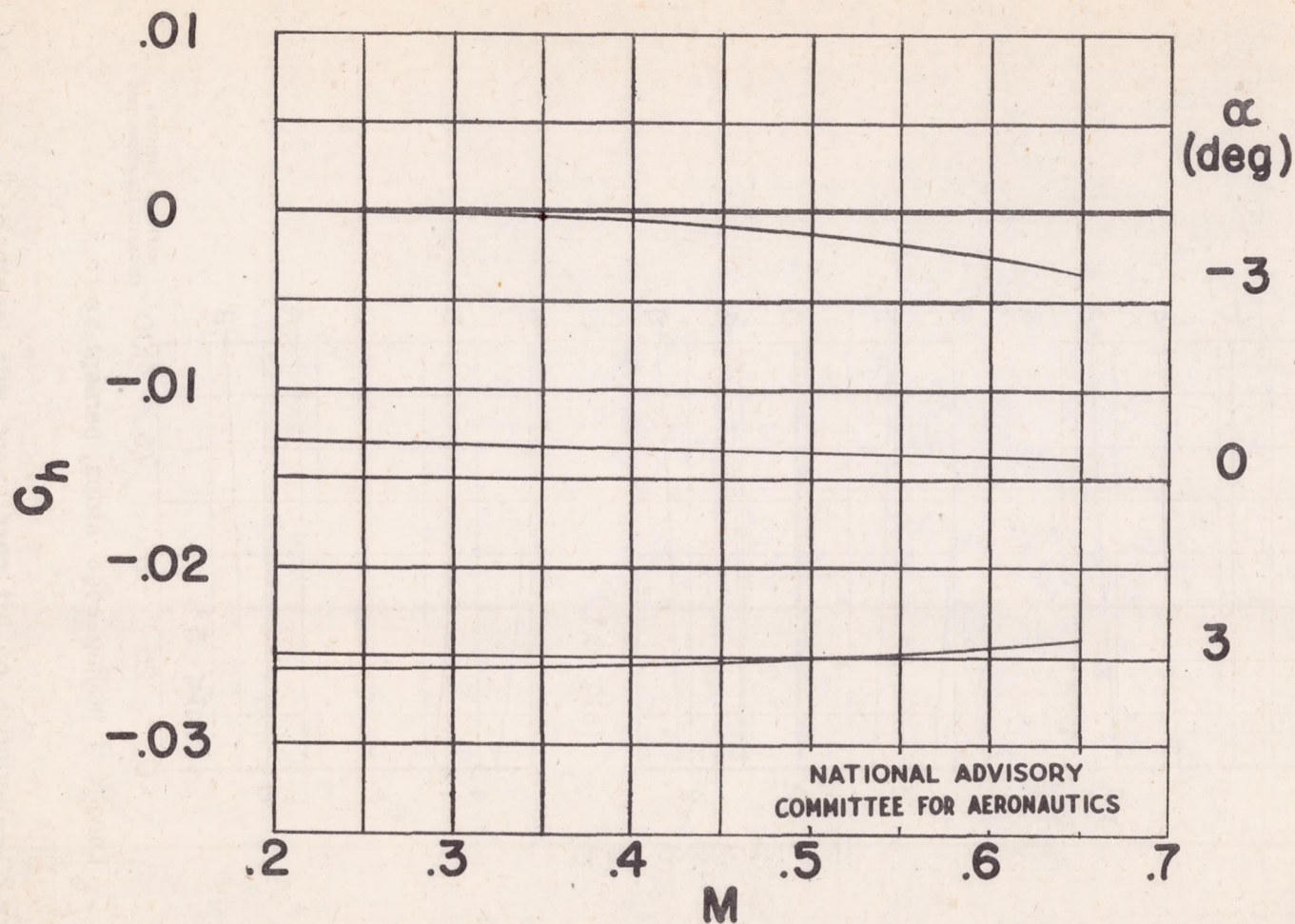
Figure 19.—Variation of elevator hinge-moment coefficient with Mach number for $\frac{1}{8}$-inch-diameter trailing-edge strips. Full span; $\delta = 0°$.

Fig. 19
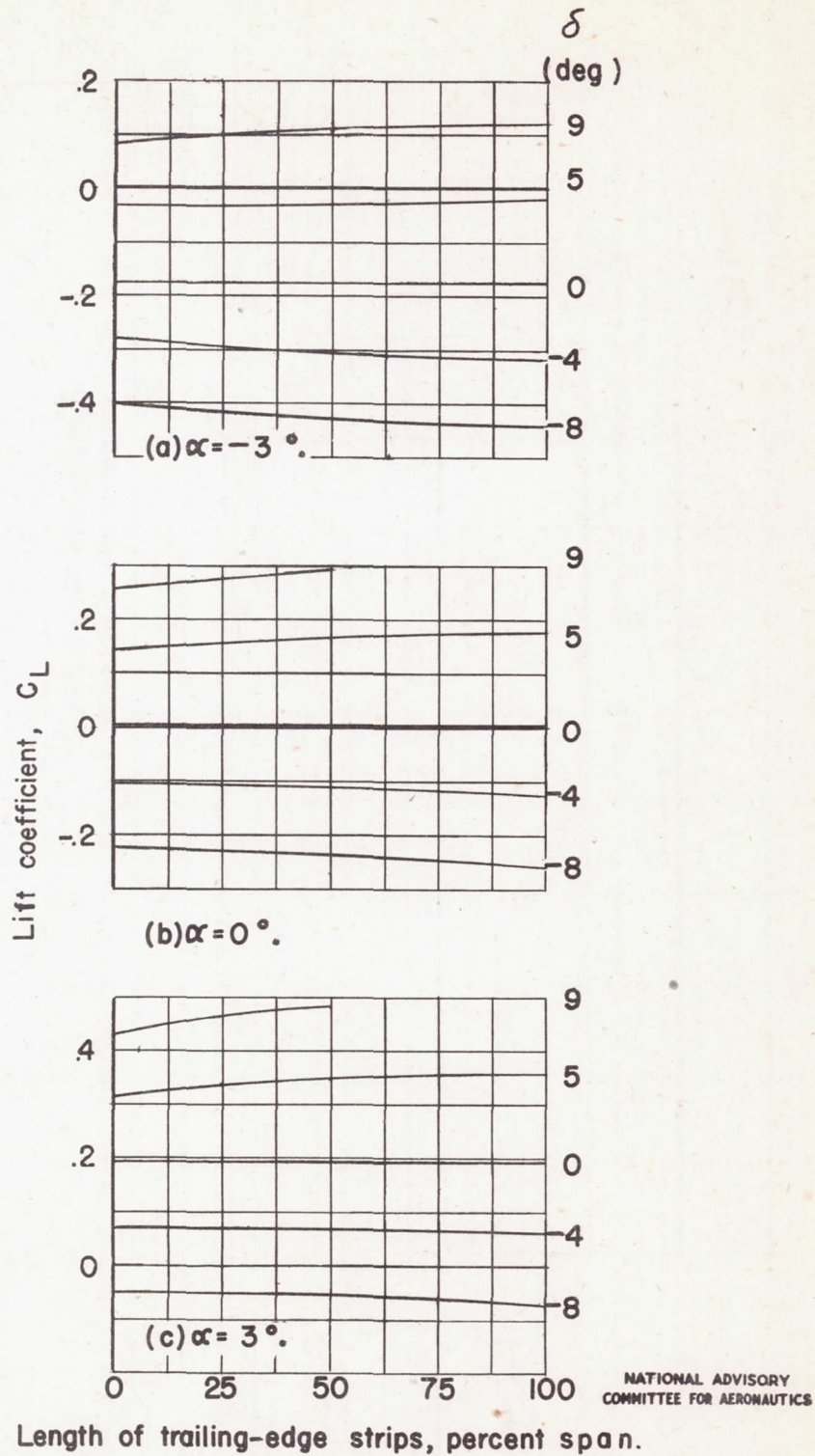
Figure 20.—Variation of lift coefficient with length of $\frac{1}{8}$-inch-diameter trailing-edge strips. M=0.35.
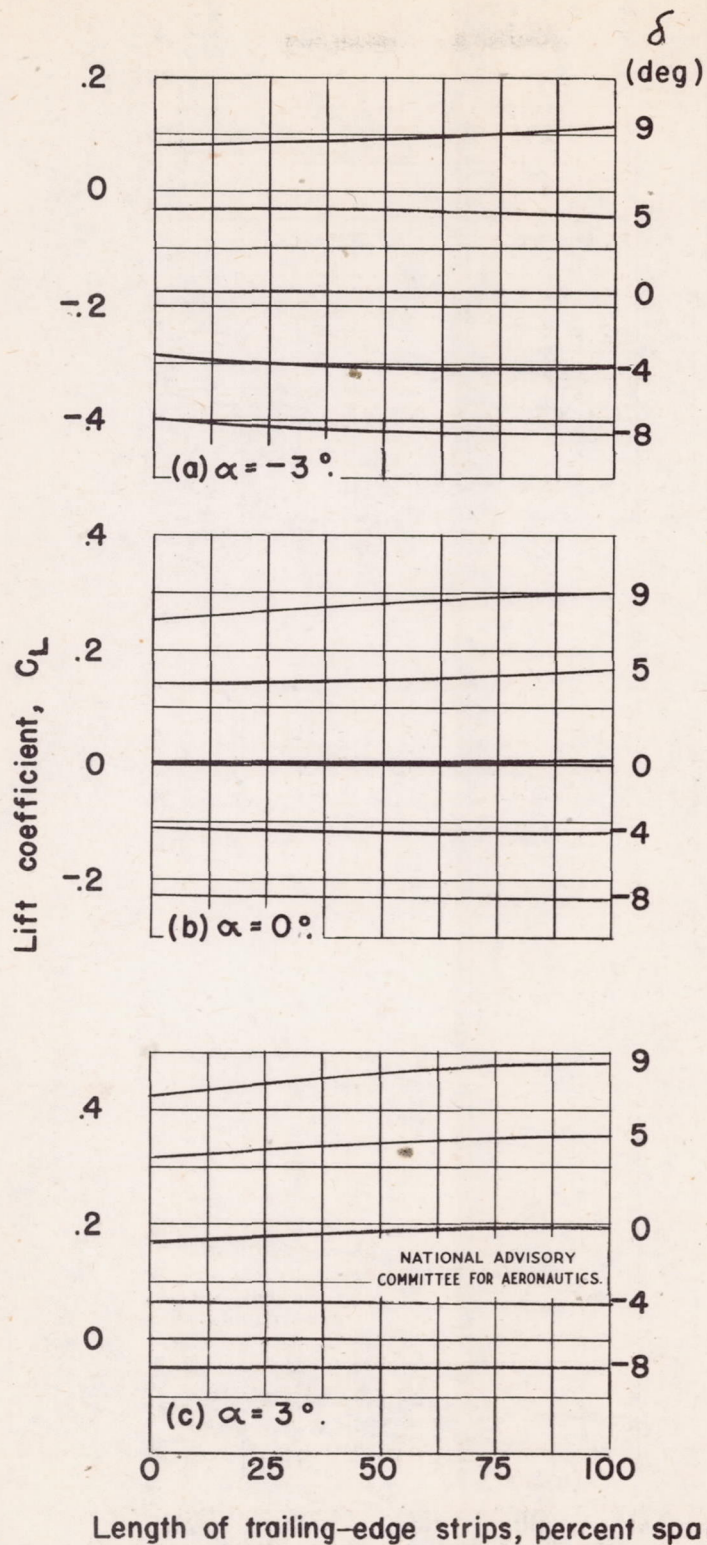
Figure 21 .— Variation of lift coefficient with length of $\frac{1}{16}$ -inch-diameter trailing-edge strips. M = 0.35.

δ
(deg)
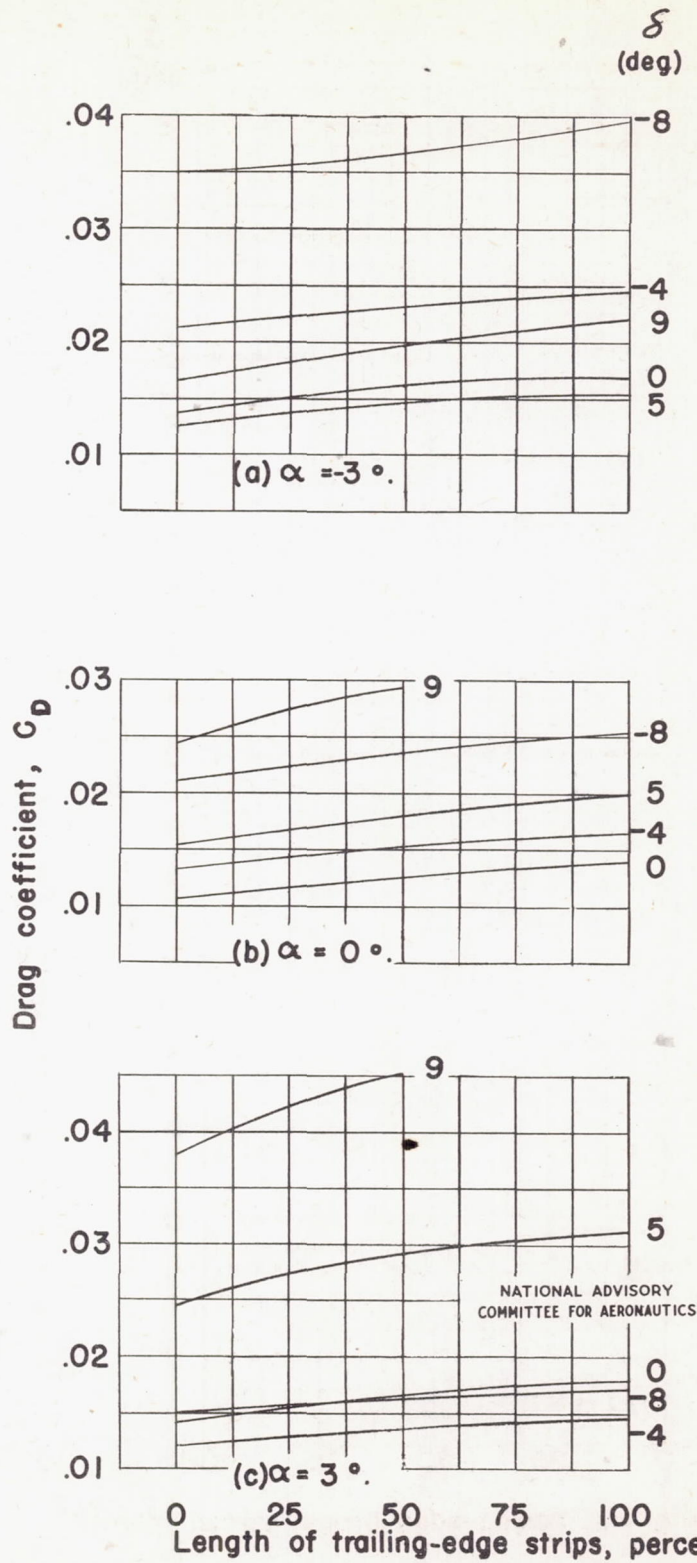
Figure 22.—Variation of drag coefficient with length of $\frac{1}{8}$-inch diameter trailing-edge strips. M=0.35.
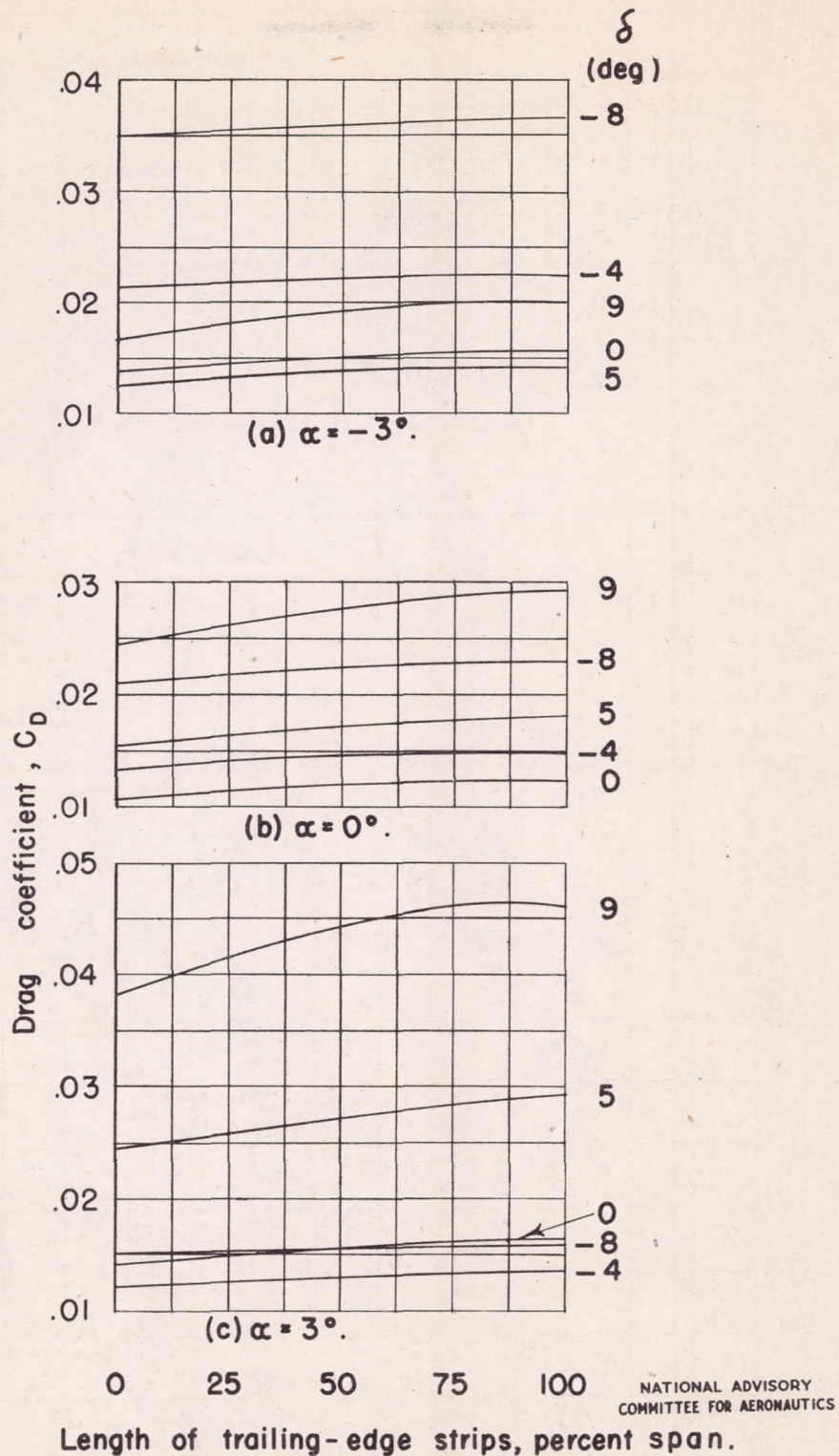
Figure 23.—Variation of drag coefficient with length of $\frac{1}{16}$-inch-diameter trailing-edge strips. M = 0.35.

(a) $\alpha = 3°$.

(b) $\alpha = 0°$.

(c) $\alpha = -3°$.
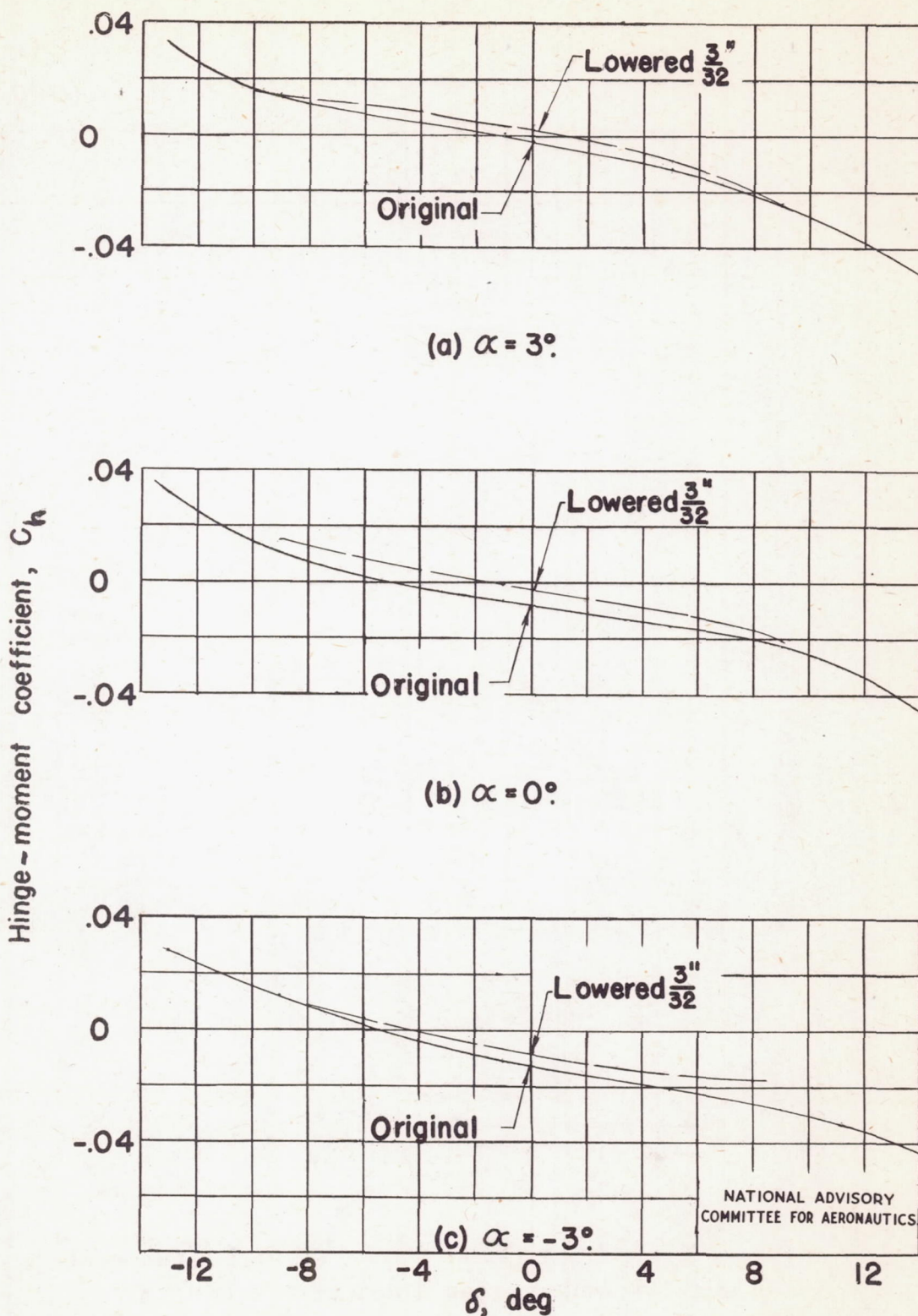
Figure 24.——Variation of hinge-moment coefficient with elevator angle for the two hinge positions. Metal elevator; M = 0.35.
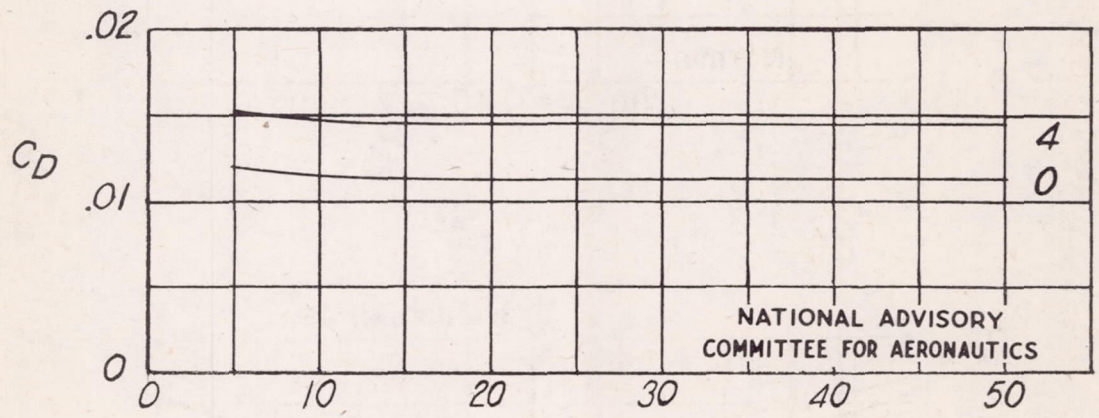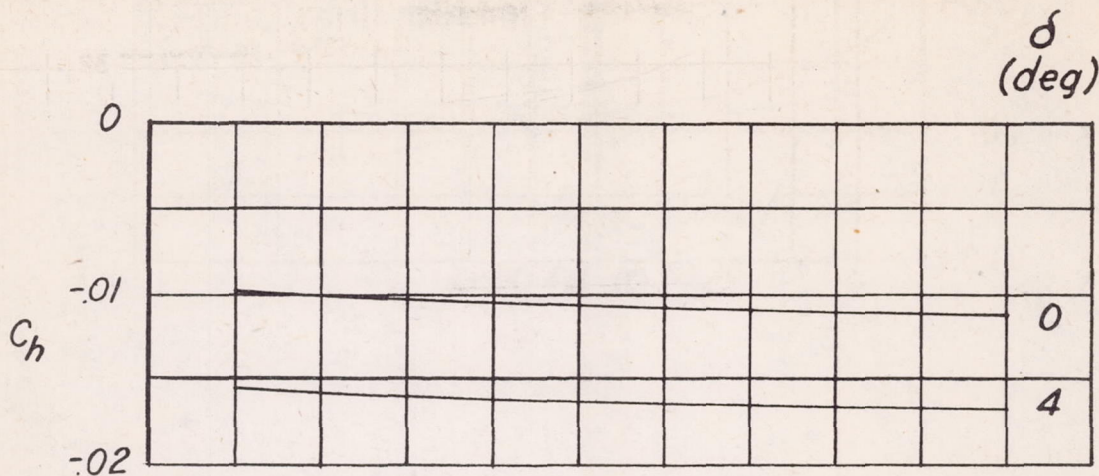
Location of transition strip, percent chord.

Figure 25.- Variation of drag and hinge-moment coefficents
with location of transition strip, upper surface. M=0.45;
α=0°. Metal elevator.
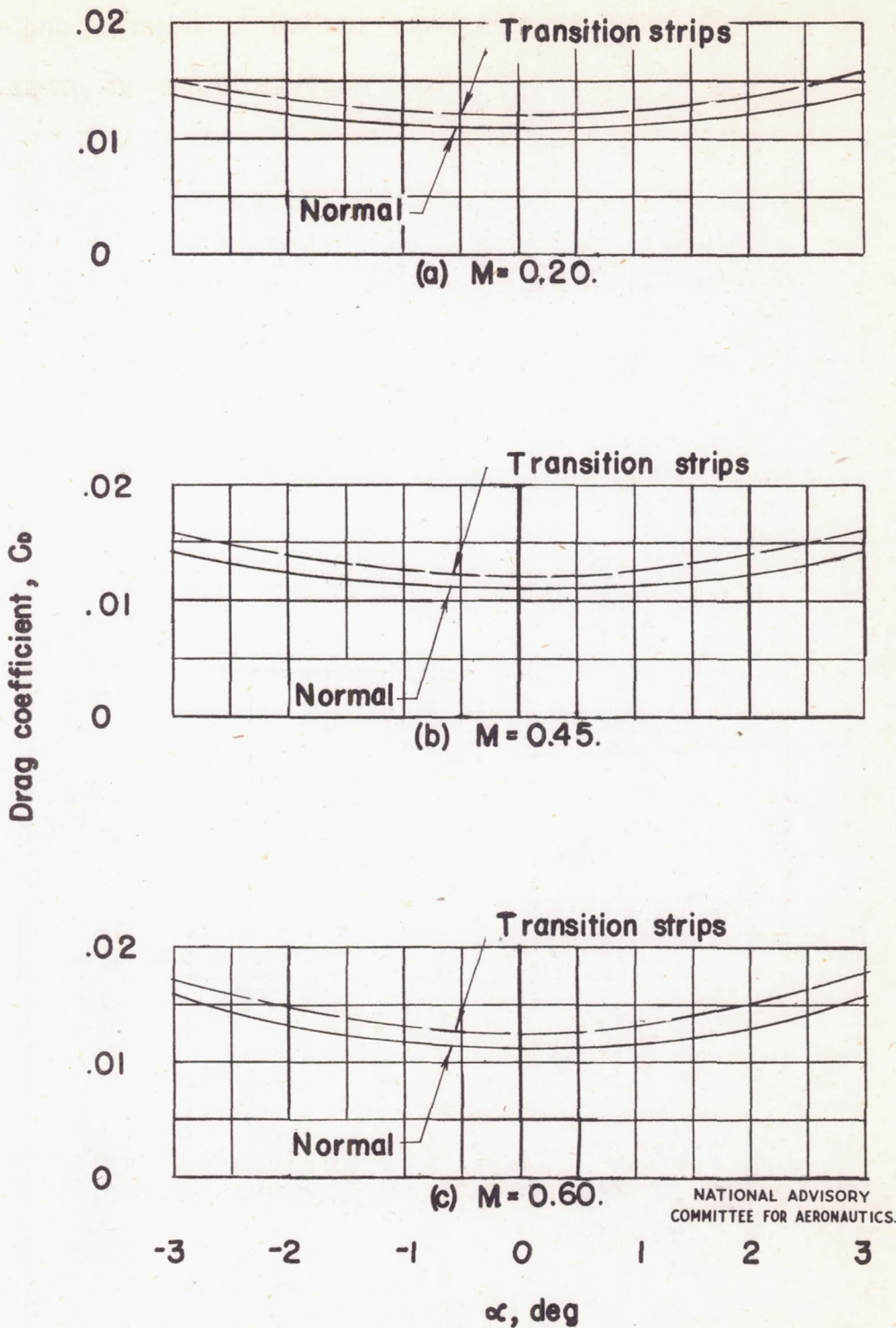
Figure 26.-Variation of drag coefficient with angle of attack for the
normal condition and with transition strips at 5 percent
chord. δ = 0°; metal elevator.

——————— From positive to negative angle

— — — — From negative to positive angle

(a) $\alpha = 3.°$

(b) $\alpha = 0.°$
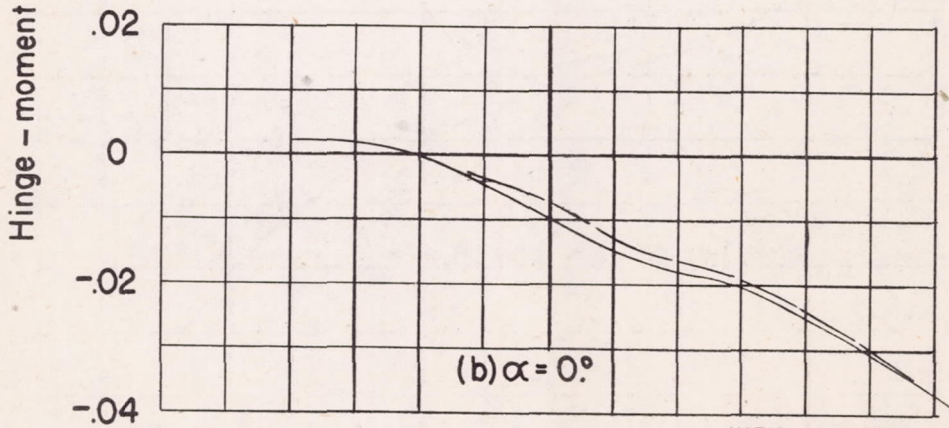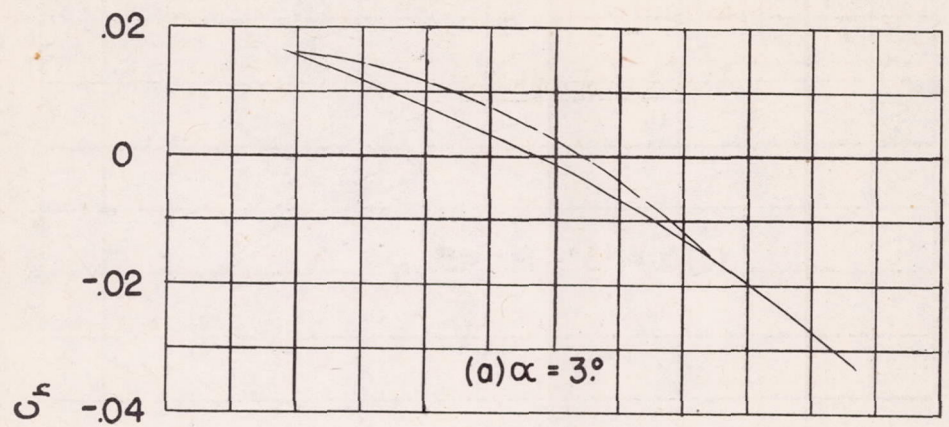
NATIONAL ADVISORY
COMMITTEE FOR AERONAUTICS

Hinge–moment coefficient, C_h

δ, deg

Figure 27.— Effect of aerodynamic hysteresis on hinge-moment coefficient. Metal-covered elevator; M = 0.50.
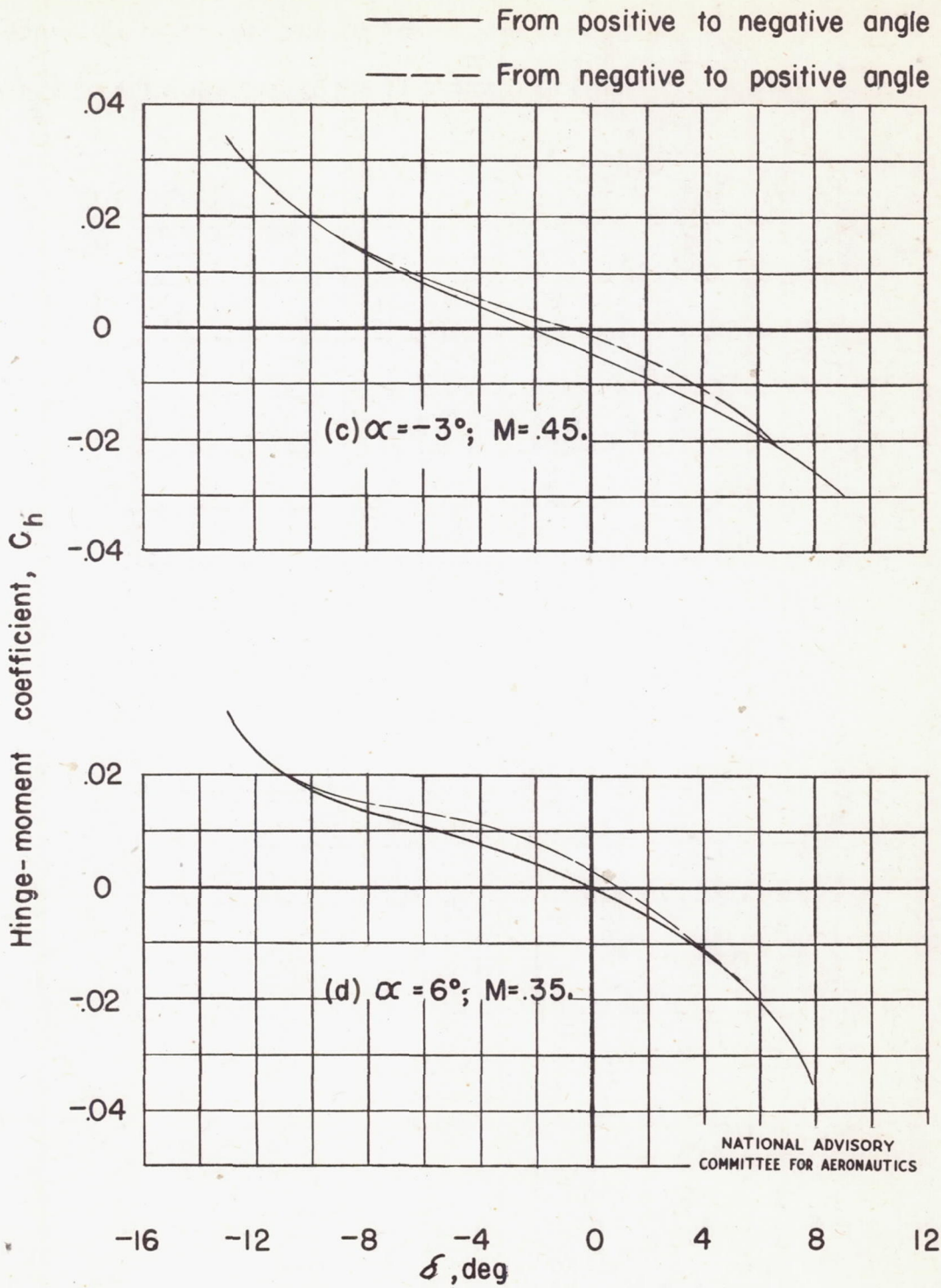
Figure 27.— Concluded.
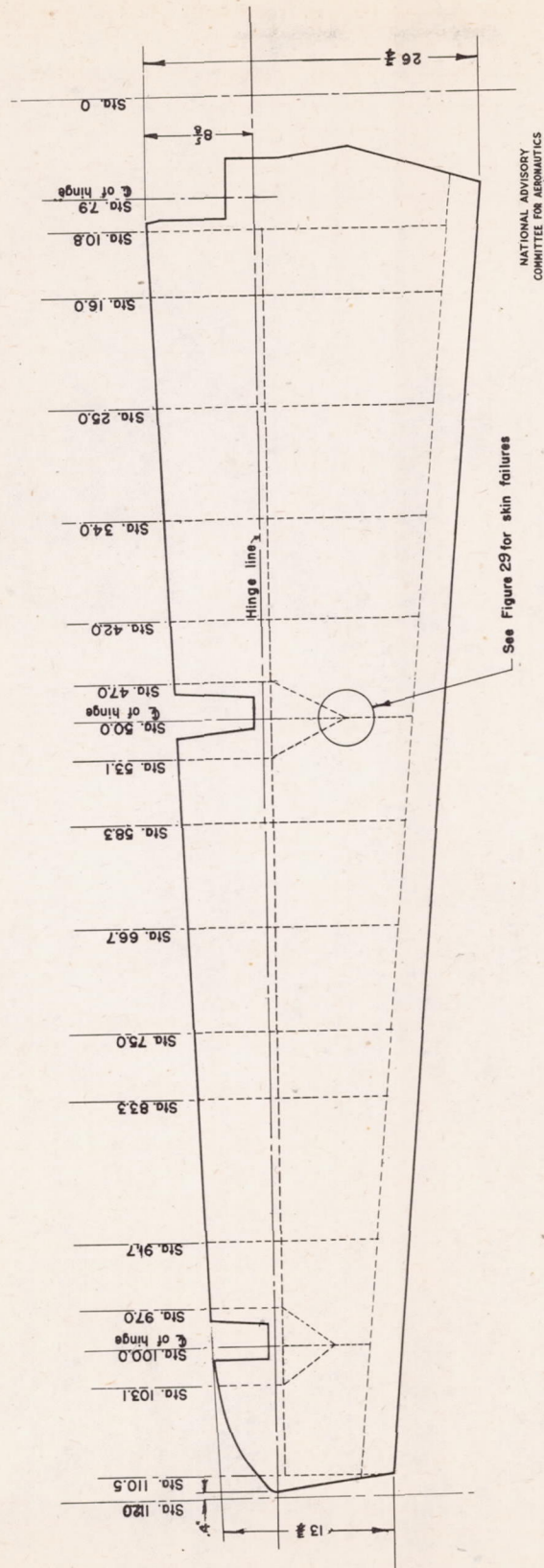
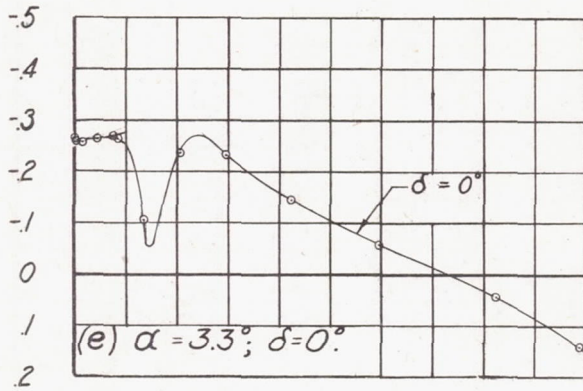Figure 28.- Detail of metal-covered elevator. All dimensions are in inches.
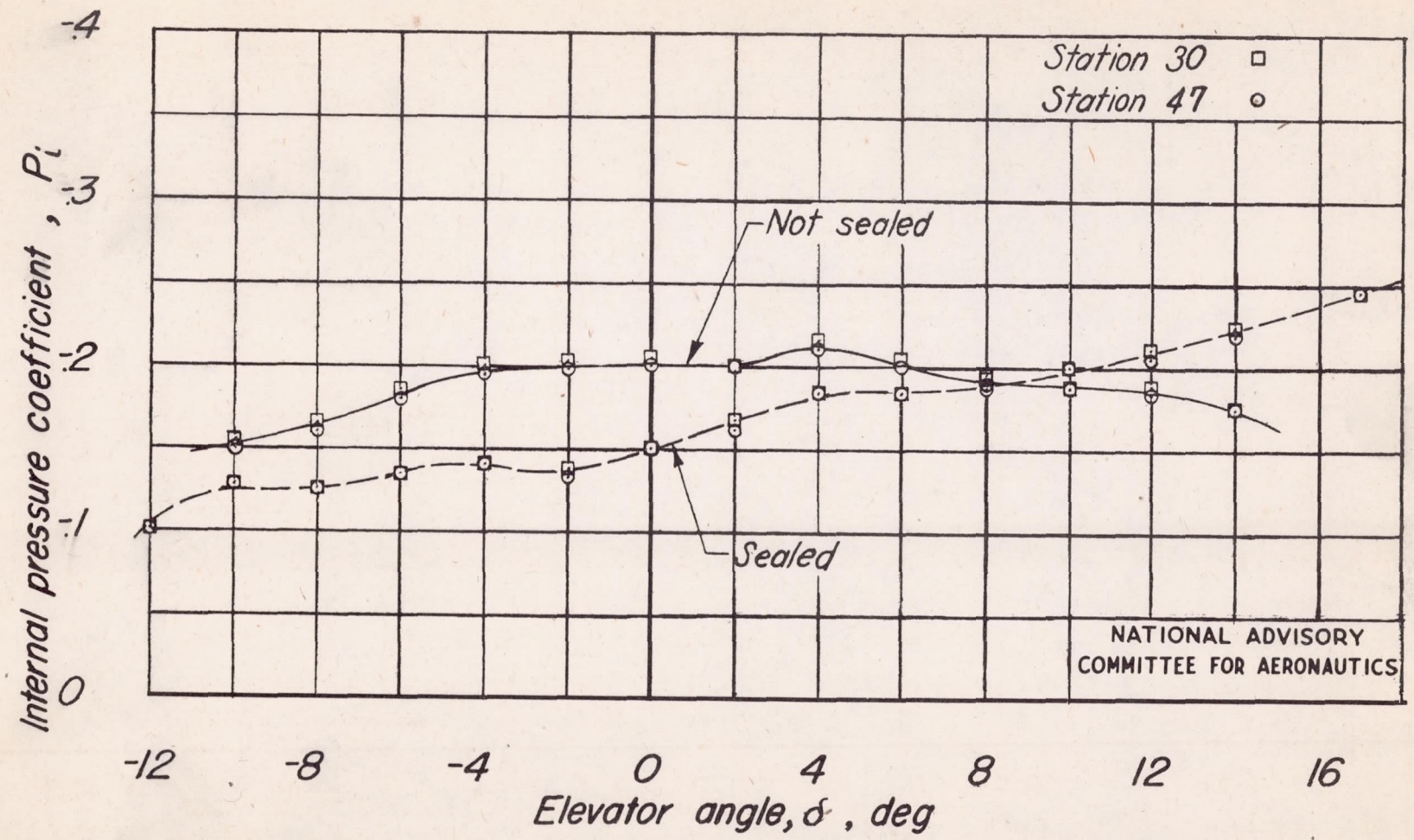
Figure 29.- Detail of upper-surface skin failure
at station 50.
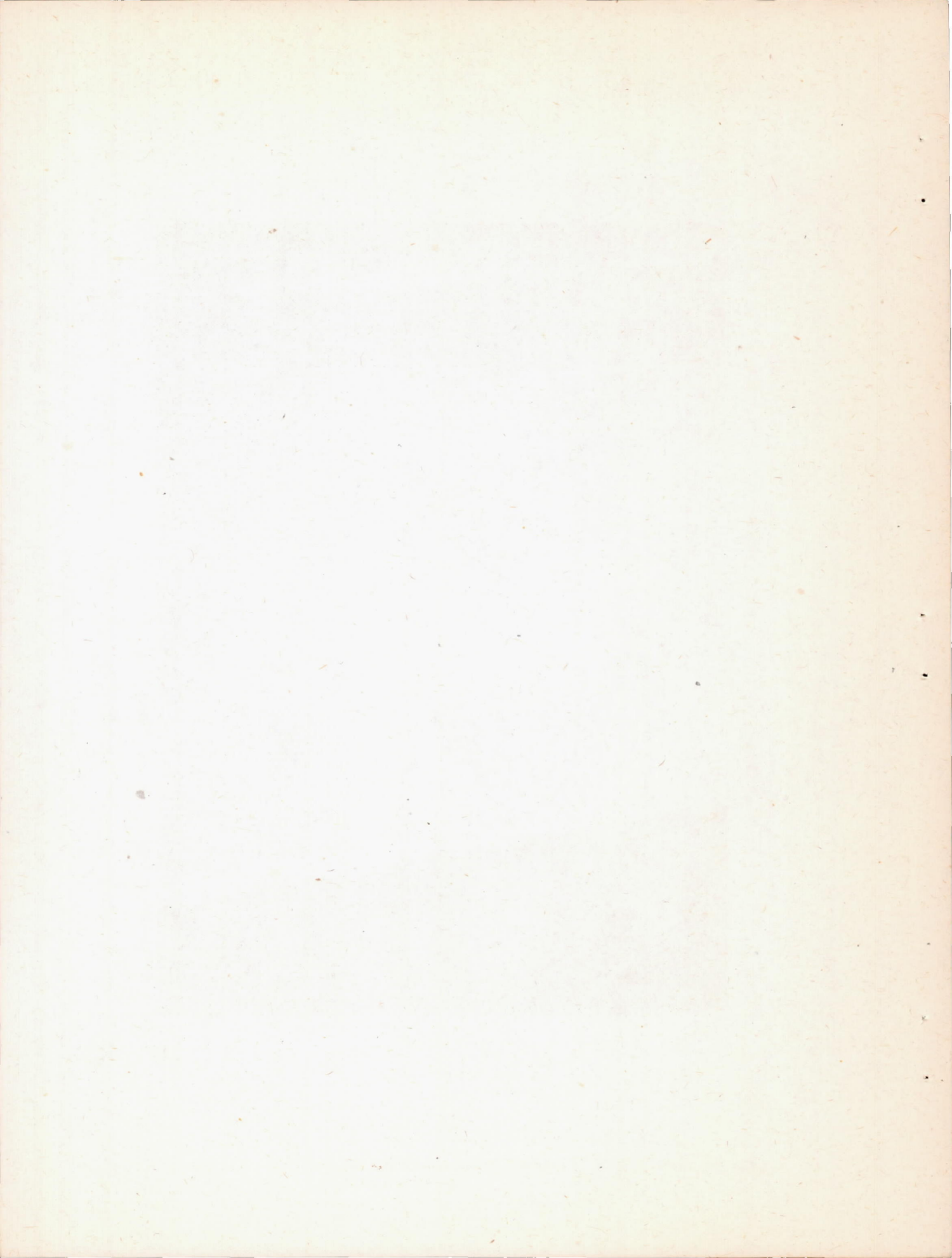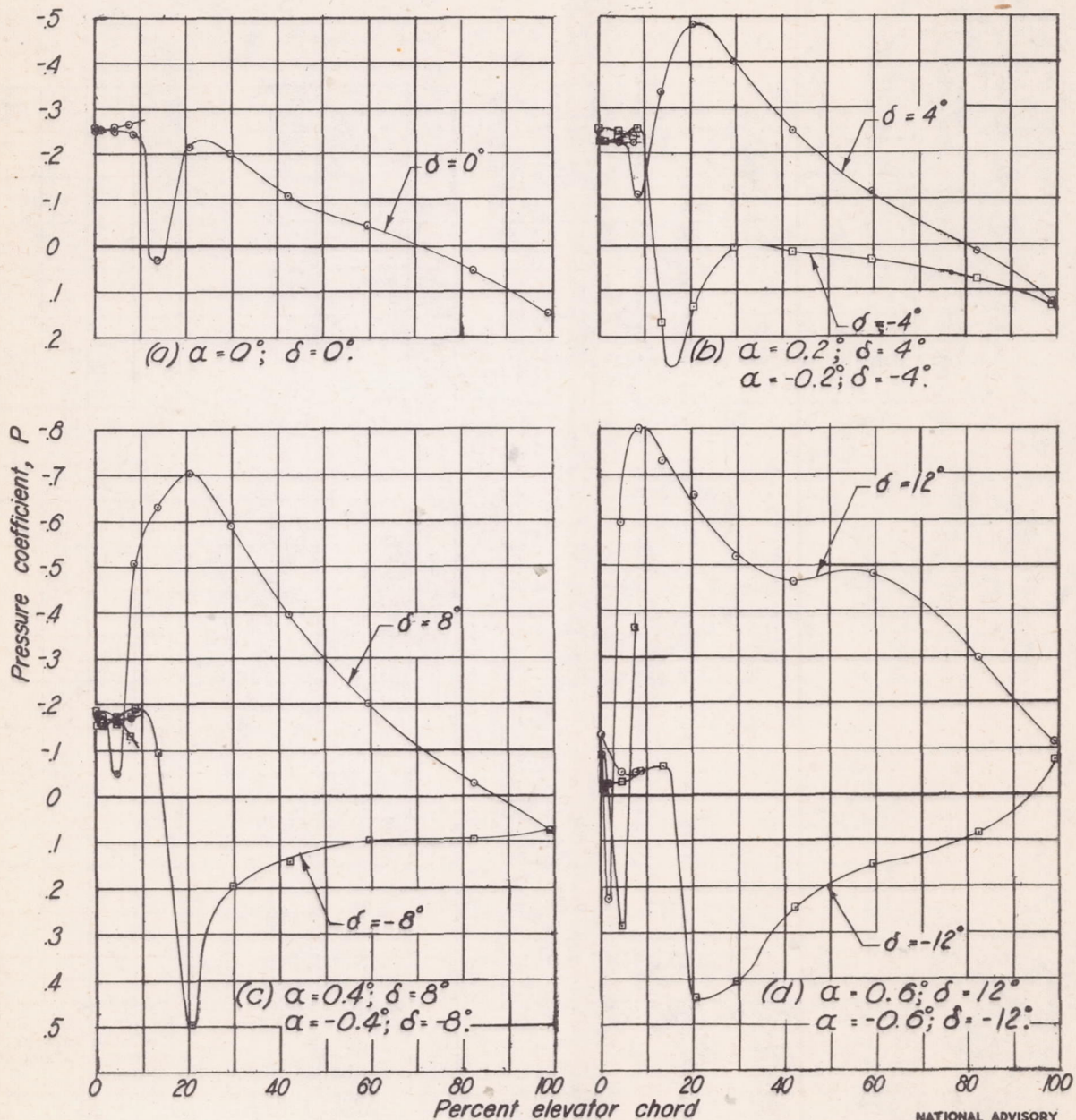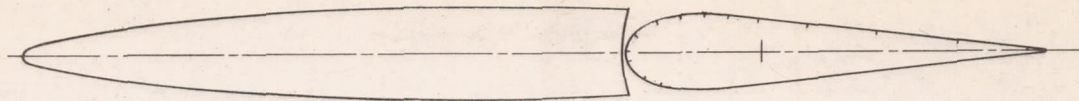
Figure 30.— Pressure distributions over the metal elevator at M = 0.20.
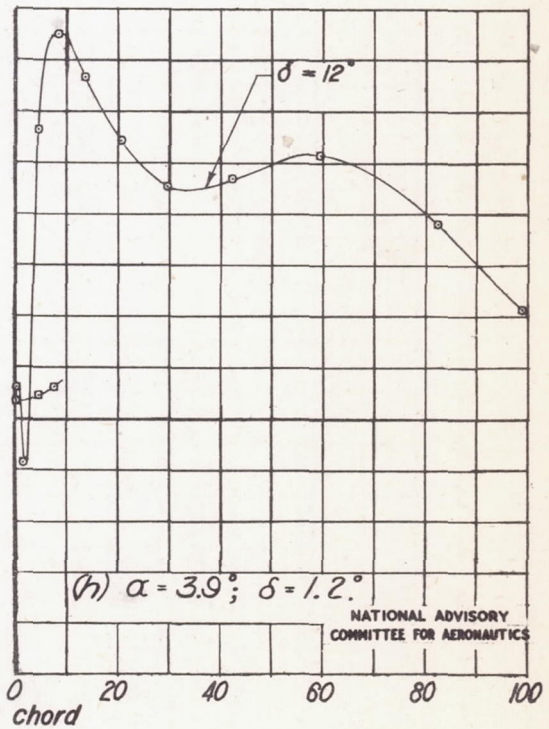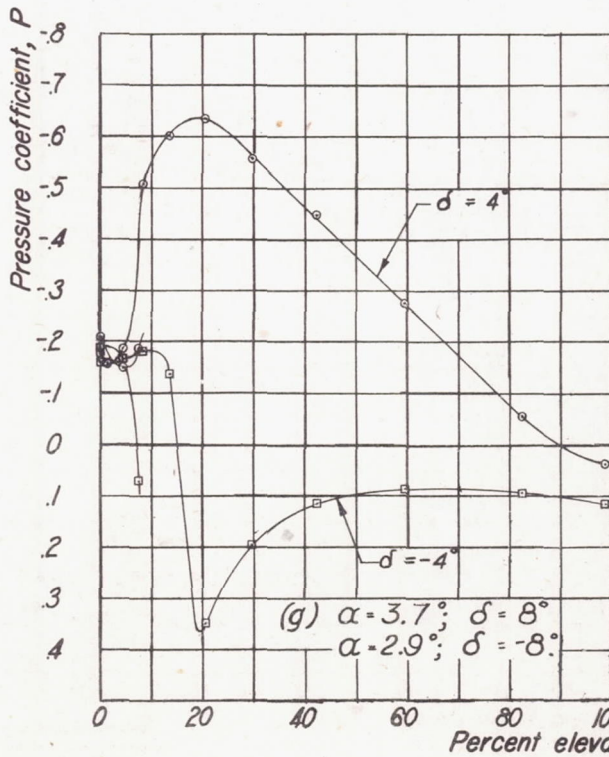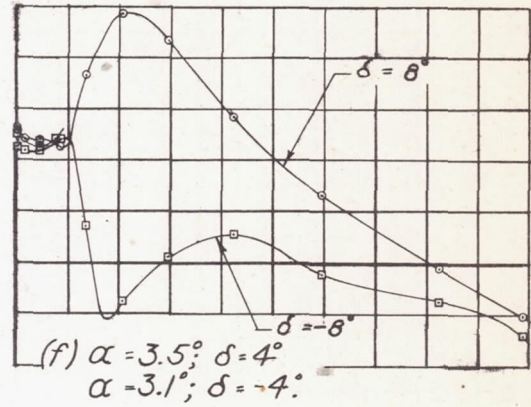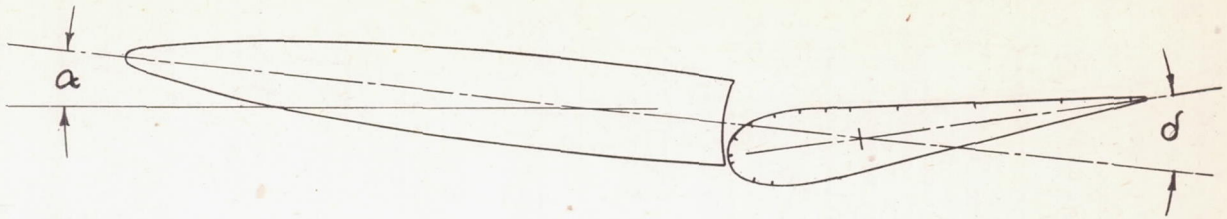
Figure 30.- Concluded.

Figure 31.- Variation of internal pressure coefficient with elevator angle. $\alpha = 0°$; $M = .20$.

Fig. 31